SJÄLVSTÄNDIGA ARBETEN I MATEMATIK

MATEMATISKA INSTITUTIONEN, STOCKHOLMS UNIVERSITET

On Some Mathematical Topics in Modeling and Analysis of Biological Systems

av

Muhammad Adnan

2012 - No 1

On Some Mathematical Topics in Modeling and Analysis of Biological Systems

Muhammad Adnan

Självständigt arbete i matematik 30 högskolepoäng, AN

Handledare: Yishao Zhou

2012

On Some Mathematical Topics in Modeling and Analysis of Biological Systems

Muhammad Adnan

January 10, 2012

Abstract

The central topic of this report is mathematical analysis of dynamical systems arising from systems biology, in particular three lower dimensional models on circadian rhythms in drosophila. Such systems have the common feature that they are large and nonlinear and many parameters and variables are nonnegative. The main issues are stability of steady state solutions, bifurcation of type Saddle node and Hopf, limit cycles and global bifurcation diagram in terms of biological parameters. The local stability of steady state and the Hopf bifurcation are carried out by the linearization together with a careful analysis using Routh-Hurwitz criterion in terms of parameters. It is found that the conclusions drawn from computer simulations in many research papers on these models are too rough to be qualified as Hopf bifurcation so a better value for the Hopf bifurcation is provided here, based on more rigorous mathematical analysis based on theory of zero locations and an extensive numerical simulation using Matlab and Mathematica. To prove the stability of the Hopf bifurcation, center manifold theorem is studied in order to compute the first Lyapunov coefficient of a dynamical system although the goal for the five dimensional model has not been achieved. In the end, descriptions on parameters resulting in saddle node bifurcation and the Hopf bifurcation are given. To make the ideas apparent for non-mathematicians the details on "bacterial growth in chemostat" are worked in most of the mathematical topics studied in this report. Some model reduction techniques are also discussed. To the best of our knowledge the theoretical results found for the five dimensional model are new.

1 Introduction

In this report, some mathematical issues frequently appearing in analysis and modelling of biological systems are discussed. The analysis of some lower (simplified) dynamical systems, in particular, arising from modelling circadian rhythms based on research papers [1, 5, 8, 13] are also presented.

Typically in biological modelling the dynamical systems are autonumous, that is, they are governed by a nonlinear differential equation of the type

$$\frac{dx}{dt} = f(x)$$

where $x \in \mathbb{R}^n$ is a state vector and $f : \mathbb{R}^n \to \mathbb{R}^n$ does not depend on t explicitly. In the topics of this thesis, x_i for example are the concentrations of different chemical substances, and f is a rational function of $x_1, x_2, x_3, ..., x_n$.

To make the thesis more accessible to readers, a short presentation on biological background relevant to the thesis is also given. A classical interesting example of the bacterial growth in chemostat (described below) is analyzed throughout the thesis to illustrate standard analysis used in biological modelling. For further details we refer to [2]. Models of circadian rhythms mainly based on the research work of Leloup and Goldbeter [5, 8] are also described briefly.

1.1 Bacterial growth in a chemostat

Let V be the constant volume of solution in culture chamber, F be (constant and equal) flows in vol/sec, e.g. m^3/s, N be bacterial population density in mass/vol, e.g. g/m^3, $C(t)$, C be nutrient concentrations in mass/vol (C_0 assumed to be constant). It is assumed that the chamber is well-mixed (i.e. continuously stirred tank reactor in chemical engineering). It is also assumed that
(i) the growth of biomass in each unit of volume is proportional to population (and to time interval length), and depends on amount of nutrient in that volume, i.e

$$N(t + \Delta t) - N(t) = K(C(t))N(t)\Delta t$$

where $K(C)$ will be discussed later.
(ii) The consumption of nutrient per unit volume proportional to increase of bacterial population, i.e.

$$C(t + \Delta t) - C(t) = -\alpha(N(t + \Delta t) - N(t))$$

due to consumption. Note that the total biomass is $N(t)V$, and the total nutrient in culture chamber is $C(t)V$. It is clear that the biomass cahnge in the time interval $\triangle t$ due to growth is

$$N(t + \Delta t)V - N(t)V = (N(t + \Delta t) - N(t))V = K(C(t))N(t)\Delta tV,$$

so contribution to $\frac{d(NV)}{dt}$ is $+K(C)NV$.

Observe that in a small interval $\triangle t$, the volume out is $F\triangle t$ which is $m^3(=(m^3/S)S)$. So, since the concentration is $N(t)(g/m^3)$, the mass out is $N(t) \pm \triangle t(g)$, thus the contribution to $\frac{d(NV)}{dt}$ is $-N(t)F$. Hence

$$\frac{d(NV)}{dt} = K(C)NV - NF$$

For $\frac{d(CV)}{dt}$ equation we have these terms $-\alpha K(C)NV$ (depletion), $-C(t)F$ (outflow) and C_0F (inflow). Thus

$$\frac{d(CV)}{dt} = -\alpha K(C)NV - C(t)F + C_0F$$

Finally, divide by constant V we obtain the following system

$$\begin{aligned}\frac{dN}{dt} &= K(C)N - NF/V \\ \frac{dC}{dt} &= -\alpha K(C)N - CF/V + C_0F/V\end{aligned}$$

A reasonable choice for $K(C)$ is

$$K(C) = \frac{K_{\max}C}{K_m + C}$$

or very usual notation

$$\frac{V_{\max}C}{K_{\mathrm{m}} + C}$$

This gives linear growth for small nutrient concentrations:

$$K(C) \approx K(0) + K'(0)C = \frac{V_{\max}C}{K_{\mathrm{m}}}$$

but saturates at $V_{\max}$ as $C \to \infty$. This expression is called *Michaelis-Menten kinetics*. When $C = K_{\mathrm{m}}$ the growth rate is $1/2$ of maximal, that is $V_{\max}/2$. This explains "m" (for middle). Therefore the two equations for the chemostat with Michaelis-Menten kinetics are

$$\begin{cases}\frac{dN}{dt} = \frac{K_{\max}C}{K_m + C}N - NF/V \\ \frac{dC}{dt} = -\alpha\frac{K_{\max}C}{K_m + C}N - CF/V + C_0F/V\end{cases} \tag{1}$$

1.2 Drosophila and Circadian Rhythms

In most kitchens the small flies that are found are Drosophila Melanogaster also called fruit fly. They are often brought in by ripened tomatoes, grapes and other perishable items from the garden. Drosophila melanogaster is a little two winged insect about 3mm long that belongs to the Diptera, the order of the flies. The drosophila egg is about half a millimeter long. Fertilization takes about one day, the embryo to develop and hatch into a worm-like larva. The larva eats and grows continuously, after two

days as a third in star larva; it moults one more time to form an immobile pupa. Over the next four days, the body is completely remodeled to give the adult winged form, which then hatches from the pupal case and is fertile within about 12 hours. Drosophila has been used as a model organism for research for almost a century, and today. One of the reasons that people work on it is because it is a small animal, with a short life cycle of just two weeks, and is cheap and easy to keep large numbers. [12]

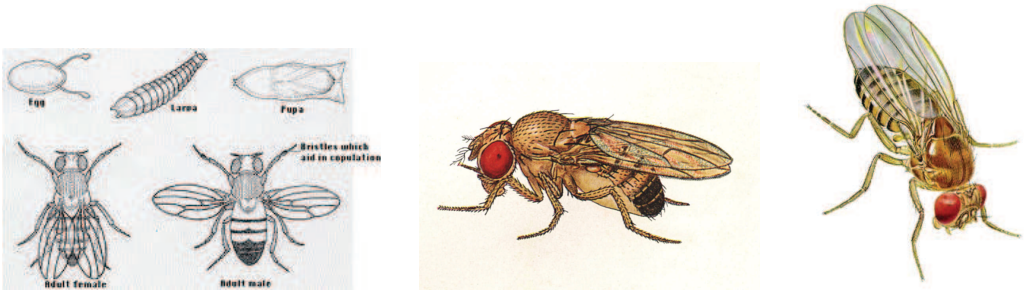

Figure 1: Pictures of the Fruit fly (Drosophila)

The most important biological rhythms are those that occur with a period close to 24 hours and that allow the organisms to adapt to periodic variations in the earth's environment. Experimental advances during the past decades have clarified the molecular bases of these rhythms. Everyone knows about his/her 24 hour sleep-wake cycle. Many other daily rhythms are exhibited by human body such as urine production, body temperature, hormone secretion and skin cell division. These kind of rhythms are observed in all kind of animals, plants and fungi, as well as in unicellular organisms and even in bacteria. As these rhythms run in the absence of external forces(cues) e.g. temperature, light intensity etc., so they reflect an endogenous oscillator inside the cells which runs at a period close to 24 hours. Circadian rhythms include the opening and closing of flowers and the nighttime increase in activity of nocturnal animals.

1.3 Organization of the thesis

The thesis is organized as follows.
In section 2, the stability analysis of steady states, stability analysis of limit cycles, stability and linearization, Lyapunov's linearization theorem, Routh-Hurwitz criterian, quasi steady state and phase portraits and global stability analysis are discussed. The knowledge of these topics is necessary to understand the theory which is discussed in the present thesis. Some examples and propositions to give brief introduction to these topics are explained. In the subsection 'quasi steady state' a more complicated example about 'Allosteric model' to give brief knowledge about this topic is also discussed. These examples include Chemostat bacterial growth, three variable model of circadian rhythms in Drosophila, five variable model of Drosphila in full and in reduced form. These proposions and examples give brief insight into these topics, so that it is very easy for a person to understand the topic, who knows very little about these topics.
Section 3 is about the center manifold theory. In this section basics of center manifold

theory, center manifold theorem and approximation theorem are given. To give clear understanding about this, the examples which clarify the use of center manifold theorem in the bifurcation analysis are included. Manifold theorem being one of the major topics which contributes in bifurcation analysis of given systems, is the motivation to include in this thesis.
The next section is the major part which was focussed at the start of the thesis. All the topics discussed in the previous sections are useful to understand the logic in this section. Here local bifurcation, global bifurcation, saddle-node bifurcation, Hopf bifurcation, Andronov-Hopf theorem are discussed with examples and figures. The five variable model of circadian rhythms in drosophila is solved numerically. The phase portraits and plots are drawn to understand the solution and the behaviour of certain parameters on the curves. Bifurcation diagrams of the circadian model are the major part of this section. A better approximation of Hopf bifurcation for five dimensional system is given here. In the end of the section some theorems and statements about the D-curve and H-curve are also given. Tangential property and convexity property are also part of this section which give another view about the bifurcation analysis. At the end a further discussion has been included, which clarify some topics which are not discussed in this thesis.

2 Stability analysis of steady states

Consider the system described by

$$\frac{dx}{dt} = f(x) \tag{2}$$

where $x(t)$ is the state vector and f is a vector having components $f_i(x_1, x_2, ..., x_n)$, for $i = 1, 2, ..., n$. If $f(c) = 0$ for all t where c is some constant vector, then it follows at once from (2) that if $x(t_0) = c$ then $x(t) = c$ for all $t \geq t_0$. Thus solutions starting at c remains there, and c is said to be an *equilibrium* or *steady state solution*. The latter is used in the biological context. It is assumed that there is no other constant solution in the neighbourhood of a *steady state solution*, that is, the steady state solutions to be studied are *isolated*.

The concept of steady state has relevance in many fields. In particular thermodynamics and economics. Steady state is more general situation than dynamic equilibrium. If a system is in steady state, then the recently observed behaviour of the system will continue in the future.

In chemistry, thermodynamics and other chemical engineering, a steady state is a situation in which all the variables are constant inspite of ongoing processes that strive to change them. For an entire system to be at a steady state, i.e. for all state variables of a system to be constant, there must be a flow through the system. One of the simplest examples of such a system is the case of a bathtub with the tap open but without the bottom plug. After some time the water flows in and out at the same rate, so the water level (state variable being volume) stabilizes and the system is at steady state.

Example 2.1. (Bacterial growth in a chemostat, [2]) Now consider the chemostat model (1). Define $\hat{c} = K_m$, $\hat{t} = \frac{V}{F}$, $\hat{N} = \frac{\hat{c}}{\alpha \hat{t} K_{max}} = \frac{K_m F}{\alpha V K_{max}}$. Make a variable change $c = c^\star \hat{c}$, $N = N^\star \hat{N}$, $t = t^\star \hat{t}$. A straight forward calculation gives the following dimensionless differential equations, after dropping stars:

$$\frac{dN}{dt} = \alpha_1 \left(\frac{C}{1+C} \right) N - N \tag{3}$$

$$\frac{dC}{dt} = -\left(\frac{C}{1+C} \right) N - C + \alpha_2 \tag{4}$$

where $\alpha_1 = \frac{V K_{max}}{F} > 0$ and $\alpha_2 = \frac{C_0}{K_m} > 0$ are two dimensionless parameters (in place of the original six). The old and new variables are related as follows

$$N(t) = \hat{N} N^\star \left(\frac{t}{\hat{t}} \right) = N^\star \left(\frac{Ft}{V} \right) \frac{K_m F}{\alpha V K_{max}}$$

$$C(t) = \hat{C} C^\star \left(\frac{t}{\hat{t}} \right) = K_m C^\star \left(\frac{Ft}{V} \right)$$

By definition, the steady state solutions $(\bar{C}, \bar{N})$satisfy

$$F(\bar{N}, \bar{C}) := \alpha_1 \left(\frac{\bar{C}}{1+\bar{C}} \right) \bar{N} - \bar{N} = 0$$

$$G(\bar{N}, \bar{C}) := -\left(\frac{\bar{C}}{1+\bar{C}} \right) \bar{N} - \bar{C} + \alpha_2 = 0$$

that is, two solutions

$$(\bar{N}_1, \bar{C}_1) = \left(\alpha_1 \left(\alpha_2 - \frac{1}{\alpha_1 - 1} \right), \frac{1}{\alpha_1 - 1} \right)$$

$$(\bar{N}_2, \bar{C}_2) = (0, \alpha_2)$$

Note that mathematically two steady states are found. However, the second solution represents a situation that is of no interest to the experimentalists, since there are no bacteria left and the nutrient is at the same concentration as the stock solution. So the first solution is more interesting in biological context. Nevertheless it does not always exist biologically. It depends on the parameters α_1 and α_2. Obviously, if $\alpha_1 < 1$, we get negative values. Since population density and concentrations must always be positive, negative values would be meaningless in the biological context as pointed in the Introduction. The conclusion is that α_1 and α_2 must be such that

$$\alpha_1 > 1, \quad \alpha_2 > \frac{1}{\alpha_1 - 1}.$$

In experiment we have to interpret these conditions back in terms of the original six parameters.

Example 2.2. (A three dimensional circadian model in drosophia [8].)
As we know several organisms exhibit circadian rhythms. It is entrained due to the 24-hour cycle of darkness and light, under certain conditions. Two proteins PER and TIM are thought to be responsible for this mechanism.
Tyson et al. in [13] introduced a new positive feedback loop into the original model, consisting of six variables. These six variables are concentrations of per and tim mRNAs, PER and TIM monomers and PER/TIM dimers in the cytoplasm and nucleus. The concentration of dimer in the cytoplasm, and in the nucleus are in equilibrium, thus the model can be reduced to three differential equations in which the state variables are the concentrations of mRNA (M) the protein (P_1) and the dimer (P_2).

$$\dot{M} = \frac{v_m}{1 + (P_2/P_c)^2} - k_m M \tag{5}$$

$$\dot{P}_1 = v_p M - \frac{k_1 P_1}{J_p + P_1 + r P_2} - k_3 P_1 - 2k_a P_1^2 + 2k_d P_2 \tag{6}$$

$$\dot{P}_2 = k_a P_1^2 - k_d P_2 - \frac{k_2 P_2}{J_p + P_1 + r P_2} - k_3 P_2 \tag{7}$$

where M is mRNA, P_1 is Monomer and P_2 is Dimer and the dots upon M, P_1 and P_2 stands for the derivative with respect to time t.
The variables have the following meanings:
M = per mRNA (messenger RNA)
P_1= monophosphorylated PER
P_2= biphosphorylated PER

Setting the functions in the right hand side to zero we can find the stationary states of the above dynamical system. After some algebraic calculation we get

$$M = \frac{v_m}{k_m(1 + (P_2/P_c)^2)} \tag{8}$$

$$r(k_d + k_3)P_2^2 + h_0(P_1)P_2 - k_a(P_1)^2(J_P + P_1) = 0 \tag{9}$$

where $h_0(P_1) = -k_a r(P_1)^2 + (k_d + k_3)(J_P + P_1) + k_2$.

Since equation (9) is a quadratic equation P_2 can be solved (because P_2 is concentration of dimer only positive solution is taken into account). Thus

$$P_2 = h_1(P_1) := \frac{-h_0(P_1) + \sqrt{h_0^2(P_1) + 4r(k_d + k_3)(J_P + P_1)k_a P_1^2}}{2r(k_d + k_3)} \tag{10}$$

Now from equation (8) we can write M in terms of P_1

$$M = h_2(P_1) := v_m P_c^2 [k_m(P_c^2 + h_1^2(P_1)]^{-1} \tag{11}$$

Putting P_2 in (10) and M in the equation (11) into $dP_1/dt = 0$ yields the following equation

$$v_p h_2(P_1) + k_1 h_3(P_1) + h_4(P_1) = 0 \tag{12}$$

where

$$h_3(P_1) = -\frac{P_1}{J_P + P_1 + rh_1(P_1)} \tag{13}$$

$$h_4(P_1) = -k_3P_1 - 2k_aP_1^2 + 2k_dh_1(P_1) \tag{14}$$

Equations (10) and (11) shows that P_2 and M are functions of P_1, i.e. they can be determined once P_1 is determined. If P_1 is positive then P_2 and M are also positive. Therefore the number of stationary states with three positive components is the same as the number of positive solution of (12) for P_1. The number of solutions of the system can only be changed if the derivative of (12) is also zero. i.e.

$$v_p\frac{dh_2(P_1)}{dP_1} + k_1\frac{dh_3(P_1)}{dP_1} + \frac{dh_4(P_1)}{dP_1} = 0 \tag{15}$$

see [10]

Example 2.3. (A simple model of circadian rhythms based on dimerization and proteolysis of PER and TIM [13]) When the dimerization is fast, then the monomer and the dimer are in equilibrium with each other, that is $P_2 = K_{eq}P_1^2$, then introduce the notations $P_t = P_1 + 2P_2$ (total protein), $m = M$, $K_{eq} = k_a/k_d$ and using the approximation $k_1 \approx (k_1 - k_2)$, the system in the previous example is reduced to the following two differential equations.

$$\dot{m} = g_1(P_t) - k_m m \tag{16}$$

$$\dot{P}_t = v_p m - k_1 g_2(P_t) - g_3(P_t) \tag{17}$$

where

$$g_1(P_t) = \frac{4P_c^2 v_m}{4P_c^2 + P_t^2(1-q)^2} \tag{18}$$

$$g_2(P_t) = \frac{qP_t}{J_P + P_t} \tag{19}$$

$$g_3(P_t) = \frac{k_2P_t}{J_P + P_t} + k_3P_t \tag{20}$$

$$q = \frac{2}{1 + \sqrt{1 + 8K_{eq}P_t}} \tag{21}$$

where m is the concentration of mRNA, P_t is the concentration of protein and k_1, k_2, k_3, k_m, v_m, v_p, P_c, J_P and K_{eq} are positive parameters. It should be noted that reduction of a model from higher dimensional to two dimensional system can be done in different ways.

The steady states can be found from the following single equation

$$v_p g_1(P_t) - k_1 k_m g_2(P_t) - k_m g_3(P_t) = 0 \tag{22}$$

because m can be determined by $g_1(P_t)/k_m$. As $P_t = P_1 + 2P_2$ is postive (P_1 and P_2 are preteins), then from the above equation it is clear that the steady state is also positive.

Example 2.4. (A five dimensional model [5]) The original Goldbeter model of *Drosophila* circadian rhythms is schematically shown in Fig.2. Here a five variable model is considered for circadian oscillations of the PER protein and per mRNA in drosophila as proposed in ([5]). It is based on negative feedback (shown in figure) exerted by a protein on the expression of its gene. This gene is expressed in the nucleus and transmitted into mRNA and then sent into the cytosol where it is degraded and translated into P_0.Then it undergoes multi phosphorylation from P_0 into P_1 and from P_1 into P_2. The fully phosphorylated form of the protein is marked up for degradation and transported into the nucleus in a reversible manner. The nuclear form of the protein P_N represses the transcription of the gene.
According to these assumptions and assuming a well-mixed system, an ordinary differential equation system for the concentrations is given by *Goldbeter* , which is:

$$\dot{M} = \frac{v_s K_I^n}{K_I^n + P_N^n} - \frac{v_m M}{k_m + M} \tag{23}$$

$$\dot{P}_0 = k_s M - \frac{V_1 P_0}{K_1 + P_0} + \frac{V_2 P_1}{K_2 + P_1} \tag{24}$$

$$\dot{P}_1 = \frac{V_1 P_0}{K_1 + P_0} - \frac{V_2 P_1}{K_2 + P_1} - \frac{V_3 P_1}{K_3 + P_1} + \frac{V_4 P_2}{K_4 + P_2} \tag{25}$$

$$\dot{P}_2 = \frac{V_3 P_1}{K_3 + P_1} - \frac{V_4 P_2}{K_4 + P_2} - k_1 P_2 + k_2 P_N - \frac{v_d P_2}{k_d + P_2} \tag{26}$$

$$\dot{P}_N = k_1 P_2 - k_2 P_N \tag{27}$$

where the subscript $i = 0, 1, 2$ in the concentration P_i are the degreee of phosphorylation of PER protein,P_N is used to indicate the concentration of PER in nucleus and M is the concentration of PER mRNA. The total quantity of PER protein, P_t is given by $P_t = P_0 + P_1 + P_2 + P_N$.

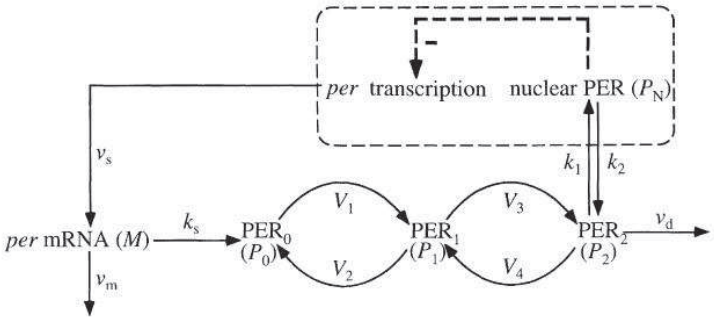

Figure 2: Scheme of the model for Circadian Rhythms in PER and per mRNA

The variables have the following meanings:
M = per mRNA (messenger RNA)
P_0 = unphosphorylated PER (period protein)
P_1= monophosphorylated PER
P_2= biphosphorylated PER
P_N= fully phosphorylated PER (referred to as simply PER)

v_s= maximum rate of M accumulation
v_m= maximum rate of M degradation
v_d= maximum rate of P_2 degradation
k_s= rate constant characterizing the synthesis of M
k_1 and k_2 = rate constant characterizing the transportation between P_2 and P_N
V_1= maximum rate of conversion, $P_0 \rightarrow P_1$
V_2= maximum rate of reverse conversion, $P_1 \rightarrow P_0$
V_3= maximum rate of conversion,$P_1 \rightarrow P_2$
V_4= maximum rate of reverse conversion, $P_2 \rightarrow P_1$
K_1= Michaelis constant for describing V_1
K_2= Michaelis constant for describing V_2
K_3= Michaelis constant for describing V_3
K_4= Michaelis constant for describing V_4
K_I= Threshold constant
n= degree of cooperativity
The details of the equations are given here, so that the background of these equations and the meaning of the constants and variables given, is understood. In 1st equation of the system $\frac{v_s K_I^n}{K_I^n + P_N^n}$ is the Hill function (inhibition), and $\frac{v_m M}{k_m + M}$ is Michaelis-Menten (Degradation). In 2nd equation of system $k_s M$ is Per synthesis: proportional to mRNA, and in 3rd and 4th $\frac{V_1 P_0}{K_1 + P_0} \pm \frac{V_2 P_1}{K_2 + P_1}, \frac{V_3 P_1}{K_3 + P_1} + \frac{V_4 P_2}{K_4 + P_2}$ is Per phosphorylation/dephosphorylation: Michaelis-Menten and $\frac{v_d P_2}{k_d + P_2}$ is Per degradation:Michaelis-Menten.In 4th and 5th $k_1 P_2 - k_2 P_N$ is Per nuclear transport: linear.
Note that the above given model is of nonlinear nature, that is impossible to solve analytically. They must be solved numerically, either implicitly or explicitly. The inhibition terms takes the form of a Hill function in 1st equation with the degree of cooperativity n, whereas $mRNA$ and protein degradation, as well as phosphorylation-dephosphorylation terms are described by Michaelis-enten functions.
The model stated above includes a negative feedback between PER and per mRNA, as shown in the figure

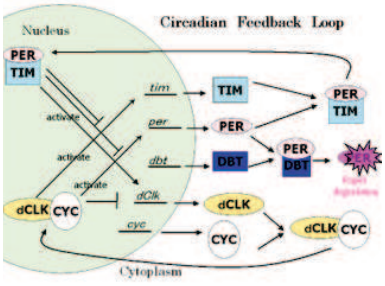

Figure 3: Feedback Loop in the system

As PER increases, the production of per mRNA decreases, causing P_0, P_1,P_2 and P_N also to decrease, but as PER decreases, the production of per mRNA increases, causing PER to increase again, and so on, which results in oscillations shown in the

figure.

By simple algeraic calculations the system of five equations system, by setting the right hand side of (23) -(27) to zero, can be written as

$$F(P_N) := v_m v_d k_2 P_N^{n+1} + (v_m v_d k_2 K_I^n - v_s K_I^n k_m k_2 k_s - v_s K_I^n v_d k_2) P_N - v_s K_I^n k_m k_1 k_d k_s = 0. \tag{28}$$

If all are solved in terms of P_N then

$$\begin{aligned}
P_2 &= \frac{k_2 P_N}{k_1}, \\
P_1 &= \frac{K_3 \left(k_1 P_2 - k_2 P_N + \frac{P_2 V_4}{K_4 + P_2} + \frac{P_2 v_d}{k_d + P_2} \right)}{-k_1 P_2 + k_2 P_N + V_3 - \frac{P_2 V_4}{K_4 + P_2} + \frac{P_2 v_d}{k_d + P_2}}, \\
P_0 &= \frac{K_1 \left(\frac{P_1 V_2}{K_2 + P_1} + \frac{P_1 V_3}{K_3 + P_1} - \frac{P_2 V_4}{K_4 + P_2} \right)}{V_1 - \left(\frac{P_1 V_2}{K_2 + P_1} + \frac{P_1 V_3}{K_3 + P_1} - \frac{P_2 V_4}{K_4 + P_2} \right)}, \\
M &= \frac{\frac{P_0 V_1}{K_1 + P_0} - \frac{P_1 V_2}{K_2 + P_1}}{k_s}.
\end{aligned}$$

If $n = 1$ the equation becomes

$$v_m v_d k_2 P_N^2 + (v_m v_d k_2 K_I - v_s K_I k_m k_2 k_s - v_s K_I v_d k_2) P_N - v_s K_I k_m k_1 k_d k_s = 0. \tag{29}$$

It can be solved explicitly. Since the discriminant

$$(v_m v_d k_2 K_I - v_s K_I k_m k_2 k_s - v_s K_I v_d k_2)^2 + 4 v_m v_d k_2 v_s K_I k_m k_1 k_d k_s > 0$$

For all parameters, we have two solutions for P_N. For simplicity we introduce $a = v_m v_d k_2 > 0$, $b = k_2 K_I (v_m v_d - v_s k_m k_s - v_s v_d)$, $c = -v_s K_I^n k_m k_1 k_d k_s < 0$. Now $F(0) = c < 0$. Then there is at most one positive solution. If $b \leq 0$, i.e.

$$-\frac{K_I k_2 [\frac{v_d}{k_s}(v_m - v_s) - v_s k_m]}{2 \frac{v_d}{k_s} v_m k_2} < 0 \tag{30}$$

$$\frac{v_d}{k_s}(v_m - v_s) - v_s k_m > 0 \quad \text{or} \quad \frac{v_d}{k_s}(v_m - v_s) > v_s k_m$$

$$\frac{v_d}{k_s} > \frac{v_s k_m}{v_m - v_s} \tag{31}$$

where $v_s < v_m$, then there is exactly one positive solution. If

$$\frac{v_d}{k_s} < \frac{v_s k_m}{v_m - v_s}, \quad \text{i.e.} \quad b > 0$$

Since $F(P_N)$ is a convex function for all P_N and $F(0) < 0$, so there exist exactly one positive solution.

To conclude that there is exactly one positive solution, we prove the following proposition.

Proposition 2.5. *There is a unique positive solution of* $F(P_N) = 0$.

Proof. Let $\bar{v} = \dfrac{v_m v_d}{k_m k_s + v_d}$. Note that $F(0) = c < 0$ and $dF(P_N)/dP_N = a(n+1)P_N^n + b$. From this if $b > 0$, or $v_s < \bar{v}$ then F is strictly increasing for $P_n \geq 0$. Hence F has a unique solution because $F(P_N) \to +\infty$ as $P_N \to \infty$. If $b \leq 0$, or $v_s \geq \bar{v}$ then the convexity of F, together with the properties $F(P_N) \to +\infty$ as $P_N \to \infty$, $F(0) < 0$, also yields that F has a unique positive solution. □

2.1 Stability and linearization

As mentioned earlier a steady state is a situation in which the system does not appear to undergo any change. However, in realistic situations there are always small unexpected disturbances. Therefore it is interesting to determine whether such deviations from steady state will lead to drastic changes. This leads to the question of stability of the steady state. There are many notions of stability. Only the following fundamental statements are considered here.

A steady state $x = c$ is said to be: *stable (in the sense of Lyapunov)* if for any positive scalar ε there exists a positive scalar δ such that $\|x(t_0) - c\| < \delta$ implies $\|x(t) - 0\| < \varepsilon$, for $t \geq t_0$;
asymptotically stable if it is stable and if in addition $x(t) \to 0$ as $t \to \infty$;
unstable if it is not stable; i.e. there exists an $x(t_0)$ with $\|x(t_0) - c\| < \delta$, $\|x(t_1)\| \geq \varepsilon$ for some $t_1 > t_0$. If this holds for every $x(t_0)$ in $\|x(t_0) - c\| < \delta$ the steady state is *completely unstable.*[3]

Now consider the linearized system

$$\dot{x} = Ax \tag{32}$$

The following theorem is essential in stability analysis. For proof we refer to [7]

Theorem 2.6 (Lyapunov's linearization theorem)**.** *If* (32) *is asymptotically stable or unstable then the steady state $x = c$ for $\dot{x} = f(x)$, where f satisfies above condtions, has the same stability property.*

According to Lyapunov's linearization theorem, the local stability can be completely determined by the linearized system as follows. Assume that $f(x) = A(x - c) + g(x)$, using $f(c) = 0$. The matrix A denotes the $n \times n$ constant matrix having elements $(\partial f_i/\partial x_j)_{x=0}$, $g(c) = 0$ and the components of g have power series expansions in $x_1, x_2, ..., x_n$ beginning with terms of at least second degree.

Example 2.7. (Continuation of Example 2.1) Computation of the partial derivatives of F and G gives rise to Jacobi matrix

$$J(N, C) = \begin{pmatrix} \dfrac{\alpha_1 C}{1+C} - 1 & \dfrac{\alpha_1 N}{(1+C)^2} \\ -\dfrac{C}{1+C} & -\dfrac{N}{(1+C)^2} - 1 \end{pmatrix}.$$

Then

$$A_1 = J(\bar{N}_1, \bar{C}_1) = \begin{pmatrix} 0 & \dfrac{\alpha_1 \bar{N}_1}{(1+\bar{C}_1)^2} \\ -\dfrac{1}{\alpha_1} & -\dfrac{\bar{N}_1}{(1+\bar{C}_1)^2} - 1 \end{pmatrix}, \quad A_2 = J(\bar{N}_2, \bar{C}_2) = \begin{pmatrix} \dfrac{\alpha_1 \alpha_2}{1+\alpha_2} - 1 & 0 \\ -\dfrac{\alpha_2}{1+\alpha_2} & -1 \end{pmatrix}$$

Now $\mathrm{tr}(A_1) = -\frac{\bar{N}_1}{(1+\bar{C}_1)^2} - 1 < 0$ and $\det(A_1) = \frac{\bar{N}_1}{(1+\bar{C}_1)^2} > 0$, so by Routh-Hurwitz property A_1 is Hurwitz. On the other hand, $\mathrm{tr}(A_2) = \frac{\alpha_1\alpha_2}{1+\alpha_2} - 2$ and $\det(A_2) = -(\frac{\alpha_1\alpha_2}{1+\alpha_2} - 1) < 0$, so A_2 is not Hurwitz.

From the above discussion we can say that since A_1 is Hurwitz then the system is stable and since A_2 is not Hurwitz so the system is not stable.

Example 2.8 (The two-dimensional circadian rhythm model.). By a straightforward calculation the Jacobi matrix is

$$J(M,P) = \begin{pmatrix} -k_m & a_{12} \\ v_p & a_{22} \end{pmatrix}$$

where

$$a_{12} = -\frac{4\left(\frac{4K_{eq}P^2(1-q)q^2)}{\sqrt{1+8K_{eq}P}} + 2P(1-q)^2\right)P_c^2 v_m}{(P^2(1-q)^2 + 4P_c^2)^2}$$

$$a_{22} = -k_3 + \frac{k_2 P}{(J_P+P)^2} - \frac{k_2}{J_P+P} + \frac{2k_1K_{eq}q^2P}{(J_P+P)\sqrt{1+8K_{eq}P}} + \frac{k_1qP}{(J_P+P)^2} - \frac{k_1q}{J_P+P}.$$

Now investigated the stability of the steady state for the parameters $v_m = 1$, $k_m = 0.1$, $v_p = 0.5$, $k_1 = 10$, $k_2 = 0.03$, $k3 = 0.1$ $K_{eq} = 200$, $P_c = 0.1$, $J_P = 0.05$ given by Tyson *et al* [13]. In this case the steady state is the only real and positive $(1.36829, 0.537769)$. First our two phase plots starting at $M(0) = 3$, $P(0) = 3.5$ and $M(0) = 1.3$, $P(0) = 0.5$ close to the steady state, respectively, for simulation length t from 0 to 50000 are shown. If phase portraits are plotted for $t \in [0, 850]$ it can be seen that the trajectory tends to a closed curve which will be called limit cycle, as claimed in [13]. Clearly the trajectory does not converge to the steady state.

However if the phase portrait for $t \in [0, 950]$ is drawn, it gives somewhat different behavior, which indicates that the trajectory leaves the closed curve.

The steady state is unstable which can be proved by Lyapunov's linearization theorem because the Jacobi matrix at this point is

$$J = \begin{pmatrix} -0.1 & -0.454213 \\ 0.5 & 0.341759 \end{pmatrix}.$$

with a positive trace. It still remains unanswered if there is a closed curve to which the trajectory does not converge, or it is a numerical round off error.

Note that it is not necessary to compute the eigenvalues because the relation between the zeros and the coefficients of the polynomial can be used. For a second degree polynomial it is easy to show that a monic polynomial is Hurwitz if and only if the coefficients are positive. Our question is as follows. Is there any similar algebraic test for checking Hurwitz property of a higher degree polynomial? If there is no parameter in the system then perhaps it is most efficient to enter the eigenvalue problem to a computer to obtain the eigenvalues. But in biological context there are many parameters, which does not make numerical solution appealing. It is also known that there is no analytic expression for zeros of higher degree polynomials. Now the root location of a polynomial in terms of the coefficients is studied here.

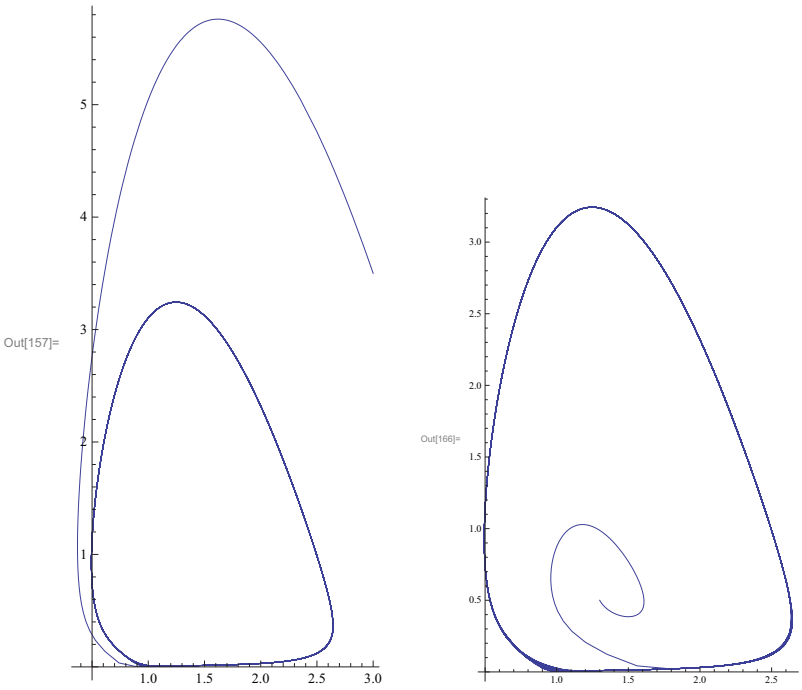

Figure 4: Phase portraits for t between 0 and 850: Left $M(0) = 3, P(0) = 3.5$, right $M(0) = 1.33, P(0) = 0.5$

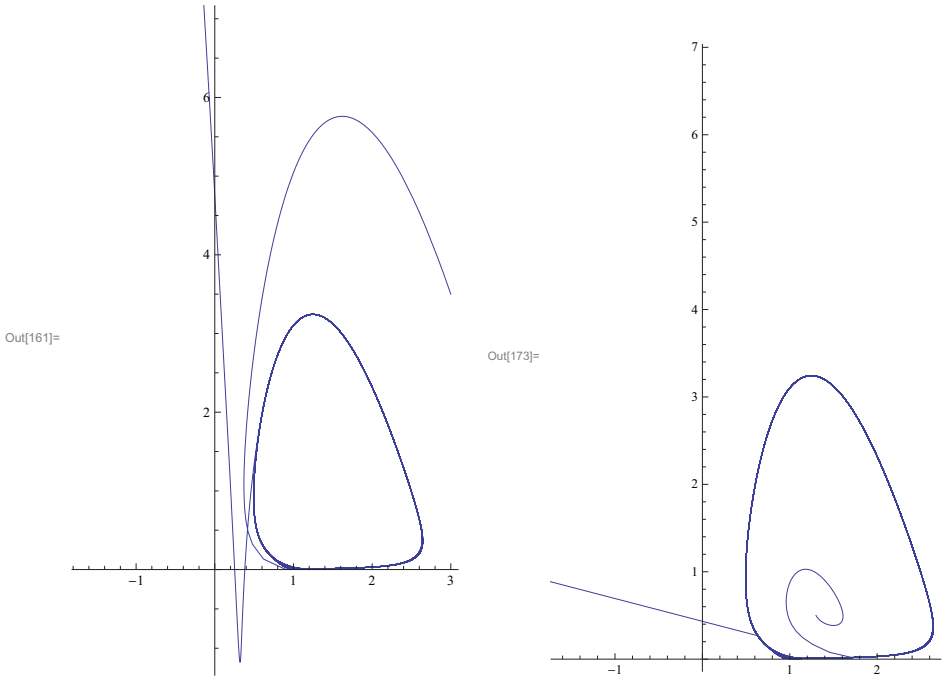

Figure 5: Phase portraits for t between 0 and 950: Left $M(0) = 3, P(0) = 3.5$, right $M(0) = 1.33, P(0) = 0.5$

2.2 Routh-Hurwitz criterion

It is demonstrated here that how Routh-Hurwitz criterion can be used in determining whether or not a real polynomial is Hurwitz (i.e. all zeros located in the left half complex plane) by examining the polynomial coefficients, rather than solving for zeros. Some propositions are also proved which will be used in the bifurcation analysis of five variable circadian model.

A necessary condition for Hurwitz polynomial is given.

Consider the real polynomial $p(s) = a_0 s^n + a_1 s^{n-1} + \cdots + a_{n-1} s + a_n$ with $a_0 > 0$

Proposition 2.9. *Suppose the real polynomial $p(s)$ is Hurwitz, then the coefficients $a_i > 0$ for $i = 1, 2, \cdots, n$.*

Proof. Without loss of generality assume that $a_0 = 1$. The polynomial $p(s)$ can be factored into the form

$$p(s) = (s + r_1) \cdots (s + r_{k_1})(s^2 + 2c_1 s + c_1^2 + d_1^2) \cdots (s^2 + 2c_{k_2} s + c_{k_2}^2 + d_{k_2}^2)$$

where the real roots are $-r_i$ for $i = 1, 2, \cdots, k_1$ and the complex roots are $-c_j \pm d_j i$ for $j = 1, 2, \cdots, k_2$ and $k_1 + 2k_2 = n$. If all of the roots are either negative or have negative real parts, i.e. $r_i > 0$ and $c_j > 0$ for all i and j. Thus, all the coefficients in the factors are positive, which implies that if $p(s)$ is expanded and simplify

$$s^n + a_1 s^{n-1} + \cdots + a_{n-1} s + a_n = 0$$

then all of the coefficients must satisfy $a_i > 0$, $i = 1, 2, 3, \cdots, n$ □

Example 2.10. Consider the differential equation

$$\frac{d^3x}{dt^3} + a_2 \frac{dx}{dt} + a_3 x = 0, \quad a_2, a_3 > 0$$

Because $a_1 = 0$, it follows from the proposition that at least one of three conditions is valid. The three conditions are (i) one eigenvalue is zero, (ii) one eigenvalue is purely imaginary,(iii) one eigenvalue lies in the right half of the complex plane.

The so-called Routh array is computed as follows:

$$\begin{array}{cccc} a_0 & a_2 & a_4 & ... \\ a_1 & a_3 & a_5 & ... \\ b_1 & b_2 & b_3 & ... \\ c_1 & c_2 & c_3 & ... \\ \vdots & & & \end{array}$$

where $b_1 = (a_1 a_2 - a_0 a_3)/a_1$, $b_2 = (a_1 a_4 - a_0 a_5)/a_1$,... $c_1 = (b_1 a_3 - a_1 b_2)/b_1$, $c_2 = (b_1 a_5 - a_1 b_3)/b_1$, ... It terminates if all the elements of the row becomes zero. Now the most important theorem is stated here.

Theorem 2.11 (Routh-Hurwitz criterion)**.** *The polynomial $p(s)$ is Hurwitz if and only if there is no sign change in the first column of the Routh array.*

Since the proof is much involved , we refer to [14].
In other words, the number of zeros on the right half complex plane is equal to the number of sign changes in the first column. This method does not compute the zeros. This is particularly useful when there are parameters involved in the coefficients.

Example 2.12 (Continuation of Example 2.3). Let $(x_M, x_{P_0}, x_{P_1}, x_{P_2}, x_{P_N})$ be a steady state of the five dimensional system. Then the Jacobi matrix evaluated at this point is

$$J = \begin{pmatrix} -\frac{k_m v_m}{(k_m + x_M)^2} & 0 & 0 & 0 & -\frac{K_I^n v_s n {P_N}^{n-1}}{(K_I^n + x_{P_N})^2} \\ k_s & -\frac{K_1 V_1}{(K_1 + x_{P_0})^2} & \frac{K_2 V_2}{(K_2 + x_{P_1})^2} & 0 & 0 \\ 0 & \frac{K_1 V_1}{(K_1 + x_{P_0})^2} & a_{32} & \frac{K_4 V_4}{(K_4 + x_{P_2})^2} & 0 \\ 0 & 0 & \frac{K_3 V_3}{(K_3 + x_{P_1})^2} & a_{44} & k_2 \\ 0 & 0 & 0 & k_1 & -k_2 \end{pmatrix}$$

where

$$a_{32} = -\frac{K_2 V_2}{(K_2 + x_{P_1})^2} - \frac{K_3 V_3}{(K_3 + x_{P_1})^2}, a_{44} = -k_1 - \frac{K_4 V_4}{(K_4 + x_{P_2})^2} - \frac{k_d v_d}{(k_d + x_{P_2})^2}.$$

Now consider the following values for the parameters
$k_2 = 1.3$, $V_1 = 3.2$, $V_3 = 5$, $k_s = 0.38$, $k_d = 0.2$, $K_1 = 2$, $K_3 = 2$, $K_I = 1$, $k_1 = 1.9$, $V_2 = 1.58$, $V_4 = 2.5$, $k_m = 0.5$, $v_d = 0.95$, $n = 4$, $K_2 = 2$, $K_4 = 2$, $v_m = .65$. Choose $v_s = 0.5$, then the steady state is

$$(1.47154, 0.705875, 0.42255, 0.286166, 0.418242)$$

and it is stable because the eigenvalues of J are

$$-4.96177, -2.19738, -0.772061, -0.114706 + 0.141076i, -0.114706 - 0.141076i.$$

For $v_s = 0.638$, the steady state is

$$(1.77304, 0.965103, 0.606842, 0.487793, 0.712928).$$

It is unstable because the eigenvalues of J are

$$-4.40777, -1.92483, -0.804351, 0.0000269168 + 0.267101i, 0.0000269168 - 0.267101i$$

Another way of checking the theorem (as given in [14]) is to make use of the determinants of the following matrices:

$$H_1 = \begin{pmatrix} a_1 \end{pmatrix}, \quad H_2 = \begin{pmatrix} a_1 & 1 \\ a_3 & a_2 \end{pmatrix}, \quad H_3 = \begin{pmatrix} a_1 & 1 & 0 \\ a_3 & a_2 & a_1 \\ a_5 & a_4 & a_3 \end{pmatrix}$$

and

$$H_n = \begin{pmatrix} a_1 & 1 & 0 & 0 & \cdots & 0 \\ a_3 & a_2 & a_1 & 1 & \cdots & 0 \\ a_5 & a_4 & a_3 & a_2 & \cdots & 0 \\ \vdots & \vdots & \vdots & \vdots & \cdots & \vdots \\ 0 & 0 & 0 & 0 & \cdots & a_n \end{pmatrix}$$

where $a_j = 0$ if $j > n$.

All the roots of the polynomial $p(s)$ are negative or have negative real part if and only if these determinants are positive. i.e.

$$\det(H_j) > 0, \quad j = 1, 2, 3, \cdots, n$$

When $n = 2$, the Routh-Hurwitz criteria simplify to $\det(H_1) = a_1 > 0$ and

$$\det(H_2) = \begin{vmatrix} a_1 & 1 \\ 0 & a_2 \end{vmatrix} = a_1 a_2 > 0$$

or equivalently $a_1 > 0$ and $a_2 > 0$.

For polynomials of degree $n = 2, 3, 4$ and 5, the Routh-Hurwitz criteria is summarized as follows.

$n = 2 : a_1 > 0$ and $a_2 > 0$.
$n = 3 : a_1 > 0, a_2 > 0, a_3 > 0$, and $a_1 a_2 > a_3$.
$n = 4 : a_1 > 0, a_2 > 0, a_3 > 0, a_4 > 0$, $a_1 a_2 > a_3$ and $a_1 a_2 a_3 > a_3^2 + a_1^2 a_4$.
$n = 5 : a_i > 0, i = 1, 2, 3, 4, 5$, $a_1 a_2 > a_3$, $a_1 a_2 a_3 + a_1 a_5 > a_3^2 + a_1^2 a_4$, and
$(a_1 a_4 - a_5)(a_3(a_1 a_2 - a_3) - a_1(a_1 a_4 - a_5)) > (a_1 a_2 - a_3)^2 a_5$
or $a_1 a_2 a_3 a_4 - a_3^2 a_4 - a_1^2 a_4^2 - a_1 a_2^2 a_5 + a_2 a_3 a_5 + 2 a_1 a_4 a_5 - a_5^2 > 0$.

The following properties are useful in bifurcation analysis .

Proposition 2.13. *1. If a real (monic) polynomial $p(s) = s^3 + a_1 s^2 + a_2 s + a_3$ has a real negative zero and a pair of purely imaginary zeros then $a_1 a_2 = a_3$ and $a_1 a_3 > 0$. Assume $a_1 a_2 = a_3$. Then if $a_1 a_3 > 0$, the polynomial has two purely imaginary zeros and a real zero; if $a_1 a_3 < 0$, the polynomial has three real zeros.*

2. A real monic polynomial $p(s) = s^5 + a_1 s^4 + a_2 s^3 + a_3 s^2 + a_4 s + a_5$ with $a_5 > 0$ has exactly one pair of purely imaginary zeros and three negative real zeros then $A_3 = 0$ but $A_1 > 0$, $A_2 > 0$; and if it has two pairs of purely imaginary zeros $A_1 = A_2 = A_3 = 0$, where $A_1 = a_1 a_2 - a_3$, $A_2 = a_1 a_2 a_3 - a_3^2 - a_1^2 a_4 + a_1 a_5$, $A_3 = (a_1 a_4 - a_5)(a_3(a_1 a_2 - a_3) - a_1(a_1 a_4 - a_5)) - (a_1 a_2 - a_3)^2 a_5$ or $A_3 = a_1 a_2 a_3 a_4 + a_2 a_3 a_5 - a_3^2 a_4 - a_1^2 a_4^2 + 2 a_1 a_4 a_5 - a_5^2 - a_5 a_1 a_2^2$.

Proof. 1. Assume that $\alpha, \beta i, -\beta i$ are zeros then

$$\alpha = -a_1, \beta^2 = a_2, \alpha\beta^2 = -a_3$$

Thus $a_1 a_2 = a_3$ and $a_1 a_3 > 0$. Now if $a_1 a_2 = a_3$, the polynomial becomes

$$s^3 + a_1 s^2 + \frac{a_3}{a_1} s + a_3 = (s + a_1)(s^2 + \frac{a_3}{a_1})$$

It is clear that there are purely imaginary zeros if $a_1 a_3 > 0$ and there are three real zeros if $a_1 a_3 < 0$.

2. Let $\alpha_1 < 0, \alpha_2 < 0, \alpha_3 < 0, \pm\beta i$ be zeros. Then we have

$$\begin{aligned}
a_1 =& -(\alpha_1+\alpha_2+\alpha_3),\\
a_2 =& \alpha_1\alpha_2+\alpha_3\alpha_1+\alpha_2\alpha_3+\beta^2,\\
a_3 =& -(\alpha_1\alpha_2\alpha_3+\alpha_1\beta^2+\alpha_2\beta^2+\alpha_3\beta^2),\\
a_4 =& (\alpha_2\alpha_3+\alpha_1\alpha_3+\alpha_1\alpha_2)\beta^2,\\
a_5 =& -\alpha_1\alpha_2\alpha_3\beta^2.
\end{aligned}$$

A straightforward calculation shows that

$$\begin{aligned}
A_1 =& -(\alpha_1+\alpha_2)(\alpha_2+\alpha_3)(\alpha_2+\alpha_3) > 0,\\
A_2 =& \alpha_1\alpha_2\alpha_3(\alpha_1+\alpha_2)(\alpha_2+\alpha_3)(\alpha_2+\alpha_3) > 0,\\
A_3 =& 0.
\end{aligned}$$

Similarly, It can be shown that if there are two pairs of purely imaginary zeros then $A_1 = A_2 = A_3 = 0$.

□

Example 2.14 (The celebrated Lorenz system). Consider the following three dimensional system

$$\begin{aligned}
\dot{x} &= \sigma(y-x)\\
\dot{y} &= \rho x - y - xz\\
\dot{z} &= -\beta z + xy
\end{aligned}$$

where $(x, y, z) \in \mathbb{R}^3$, $\sigma, \beta, \rho > 0$ are parameters. It is easy to prove that $(0, 0, 0)$ is the only one equilibrium point when $\rho < 1$, and the system possesses two additional equilibrium points $(\sqrt{\beta(\rho-1)}, \sqrt{\beta(\rho-1)}, \rho-1)$ and $(-\sqrt{\beta(\rho-1)}, -\sqrt{\beta(\rho-1)}, \rho-1)$ when $\rho > 1$. Hence the linearized system matrices at these equilibrium points is

$$\begin{pmatrix} -\sigma & \sigma & 0\\ \rho & -1 & 0\\ 0 & 0 & -\beta \end{pmatrix} \quad \text{respectively} \quad \begin{pmatrix} -\sigma & \sigma & 0\\ 1 & -1 & \pm\sqrt{\beta(\rho-1)}\\ \mp\sqrt{\beta(\rho-1)} & \mp\sqrt{\beta(\rho-1)} & -\beta \end{pmatrix}$$

and the characteristic polynomials are

$$\chi_0(\lambda) = (\lambda+\beta)(\lambda^2+(\sigma+1)\lambda+\sigma(1-\rho)) = 0$$

and

$$\chi_1(\lambda) = \lambda^3+(\sigma+\beta+1)\lambda^2+(\rho+\sigma)\beta\lambda+2\sigma\beta(\rho-1) = 0$$

respectively. It is also easy to show that $\chi_0(\lambda)$ has three real zeros when $\rho > 0$, and all are negative when $\rho < 1$, but one is positive when $\rho > 1$. Now it is shown that $\chi_1(\lambda)$ possesses one real negative zero and two complex conjugate zeros when $\rho > 1$, and that the complex conjugate zeros are purely imaginary if $\rho = \frac{\sigma(\sigma+\beta+3)}{\sigma-\beta-1}$.

Since $\chi_1(0) = 2\sigma\beta(\rho-1) > 0$ and $\chi_1(\lambda) \to -\infty$ as $\lambda \to -\infty$, there is at least one negative real zero.

By a straightforward calculation the first column of the Routh array can be found:

$$1, \sigma + \beta + 1, \frac{\beta(\rho(\beta + 1 - \sigma) + \sigma(\sigma + \beta + 3))}{\sigma + \beta + 1}, 2\sigma\beta(\rho - 1)$$

The case where $\rho > 1$is considered now. It is seen that the third term is the only one that can change the sign. Thus if

$$\rho(\beta + 1 - \sigma) + \sigma(\sigma + \beta + 3) > 0 \Leftrightarrow \rho > \frac{\sigma(\sigma + \beta + 3)}{\sigma - \beta - 1}$$

Then there is no sign change, assuming $\sigma > \beta + 1$. Hence $\chi_1(\lambda)$ is Hurwitz. If $\rho < \frac{\sigma(\sigma + \beta + 3)}{\sigma - \beta - 1}$ then there are two sign changes, thus there are two zeros on the right half plane. If assume $\sigma < \beta + 1$ then there is no sign change. Again the polynomial is Hurwitz. By Proposition 2.13 there is a pair of purely imaginary zeros if and only if

$$\rho = \frac{\sigma(\sigma + \beta + 3)}{\sigma - \beta - 1}$$

because $\sigma + \beta + 1 > 0$, and $2\sigma\beta(\rho - 1) > 0$. Now zeros depend on coefficient continuously, hence there is a pair of complex conjugate zeros if ρ is increased or decreased.

Example 2.15 (Continuation of Example 2.4). Now check the conditions for $v_s = 0.638$ with the parameters considered before. The reason why this value is picked, is due to the statement made by Goldbeter that a Hopf bifurcation occurs at this point. Our calculation shows that the characteristic polynomial of J has

$$a_5 = 0.486865, a_4 = 0.968316, a_3 = 7.33274, a_2 = 13.6488, a_1 = 7.1369.$$

Then

$$A_1 = 90.0776, A_2 = 614.669, A_3 = -0.256484,$$

and the sign in the first column of the Routh array $+, +, +, +, , -, +$ Thus there are two eigenvalues in right half plane, which was shown earlier. By Proposition 2.13, there is no purely imaginary eigenvalues.

We summarize the standard analysis of root location as follows:

1. Two necessary but not sufficient conditions that all the roots have negative real parts are
   (a) All the polynomial coefficients must have the same sign.
   (b) All the polynomial coefficients must be nonzero.
2. If condition 1. is satisfied, then compute the Routh-Hurwitz array and count the sign change. If the sign is preserved in the first column of the Routh array then the polynomial is Hurwitz.

Finally, the following remarks are:

1. Special Case 1: The first element of a row is zero, but some other elements in that row are nonzero. In this case, simply replace the zero element by "e", complete the table development, and then interpret the results assuming that "e" is a small number of the same sign as the element above it. The results must be interpreted in the limit as e tends to 0.

2. Special Case 2: All the elements of a particular row are zero. In this case, some of the roots of the polynomial are located symmetrically about the origin of the s-plane, e.g., a pair of purely imaginary roots. The zero row will always occur in a row associated with an odd power of s. The row just above the zero row holds the coefficients of the auxiliary polynomial. The roots of the auxiliary polynomial are the symmetrically placed roots. Be careful to remember that the coefficients in the array skip powers of s from one coefficient to the next.

2.3 Phase portraits and global stability from local information

Stability as large can be established by using Lyapunov function $V(x)$ together with the property that $V(x) \to \infty$ as $\|x\| \to \infty$. Since energy dissipates through friction, it can be taken as a Lyapunov function when modelling mechanical systems. For biological systems, however, there is no obvious way of choosing a suitable Lyapunov function. Instead phase portraits are used.

This is illustrated by working on the Chemostat model Example 2.1:- Now a days vector field plots can easily be drawn by any computer algebra program (look at the plot at the end of this example). Otherwise it can be sketched by studying the nullclines, that is all curves from $dN/dt = 0$ (N-nullclines), $N = 0$ and $C = 1/(\alpha_1 - 1)$, and $dC/dt = 0$ (C-nullclines), $N = (\alpha_2 - C)(1 + C)/C$. Details are provided in [2] 5.10.

It is already known that the solutions that start close to the positive steady state $(\bar{N}_1, \bar{C}_1)$ approach it and that start close to the other steady state diverge from it.

It is showed here that there is an invariant subset where the trajectories that start at any point on it will never leave it. And more important all the trajectories (except those that start with $N(0) = 0$ converge to it. It is observed from the vector field plot that the trajectories will approach to a line $N + 3C - 3 = 0$, corresponding to the case $\alpha_1 = 3, \alpha_2 = 1$. Thus the invariant set is the line

$$N + \alpha_1 C - \alpha_1 \alpha_2 = 0,$$

that is the line passing through the two steady states and it also passes through $(\alpha_1\alpha_2, 0)$. For any solutions, consider the function $z(t) = N(t) + \alpha_1 C(t) - \alpha_1\alpha_2$ and consequently, by a simple calculation

$$dz/dt = dN/dt + \alpha_1 dC/dt = -z$$

implying that

$$z(t) = z(0)e^{-t}.$$

Thus $z(t) = 0$ for all $t > 0$ if $z(0) = 0$ which is invariance, and in general $z(t)$ tends to 0 as $t \to \infty$. In other words, solutions tend to the line.

Uniqueness of solutions implies that no trajectories can cross the line. Suppose a trajectory starts, and remains on top of (under) the line and with $N(0) > 0$. Since the trajectory gets close to the line, and must stay in the first quadrant, it will either converge to the the stable steady state from the northwest of it will eventually enter

the region with the northwest arrow, at which it must have turned and start moving to the stable steady state. In conclusion every trajectory converges.

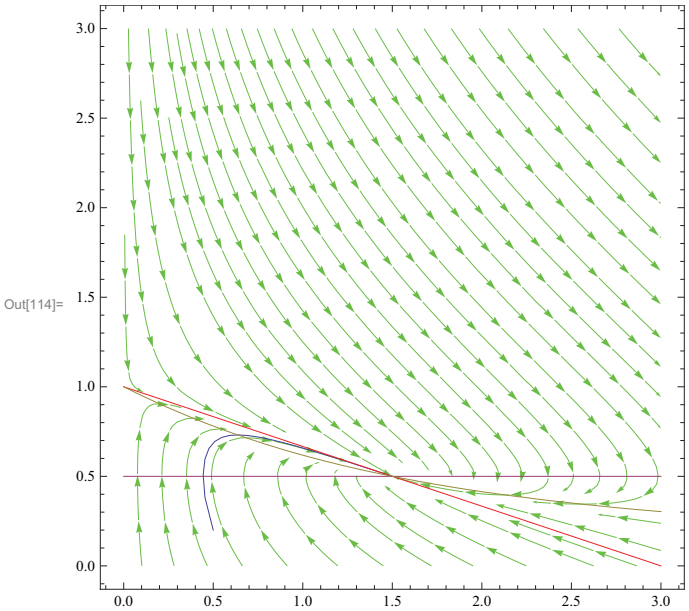

2.4 Quasi-steady-state

A full analysis of systems with two variables using phase-plane methods can be proceeded. However, many models do have more than two variables. It is common to make further assumption so that the system can be reduced to two dimensional. For example small molecules such as glucose or other nutrients are typically found in concentrations much higher than those of the receptors. So it could be argued that receptors are always working at maximal capacity, so that their occupancy rate is virtually constant. This assumption leads to the *quasi-steady-state* hypothesis (setting part of $\dot{x_1}, \dot{x_2}, \dot{x_2}, ..., \dot{x_n}$ to zero) and permits further simplification.

A close look at derivation of Michaelis-Menten kinetics is taken before proceeding. It is well-known that many biological phenomena exhibit saturating kinetics. For example in bacterial growth in chemostat described above it was assumed that for low levels of the nutrient concentration c, bacterial growth rate is roughly proportional to c. At high levels, this rate approaches a constant value $K_{\max}$.

In biochemistry, Michaelis-Menten kinetics is one the simplest and best-known models of enzyme kinetics. It is given by

$$K(C) = \frac{K_{\max} C}{K_m + C}$$

where $K_{\max}$ represents the maximum rate achieved by the system, at maximum substrate concentration. The constant K_m is the substrate concentration at which the reaction rate is half of $K_{\max}$. Note that biochemical reactions involving a single substrate are often assumed to follow Michaelis-Menten kinetics, regardless the models underlying assumptions.

Now quasi-steady state approximations in Michaelis-Menten reactions is used. Consider the following system derived from an enzymatic reactions, see [2]

$$\frac{dc}{dt} = -k_1 rc + (k_{-1} + k_1 c)x_1$$
$$\frac{dx_1}{dt} = k_1 rc - (k_{-1} + k_2 + k_1 c)x_1$$

where c is the concentration of an external nutrient molecule, and x_1 is the concentration of a nutrient-receptor complex. The quasi-steady state hypothesis yields that

$$\frac{dx_1}{dt} \approx 0$$

i.e.

$$k_1 rc - (k_{-1} + k_2 + k_1 c)x_1 = 0$$

which is

$$x_1 = \frac{k_1 rc}{k_{-1} + k_2 + k_1 c} = \frac{rc}{k_n + c} \tag{33}$$

where $k_n = (k_{-1} + k_2)/k_1$. Let $K_{\max} = k_2 r$ we obtain

$$\frac{dc}{dt} = -\frac{K_{\max} c}{k_n + c}. \tag{34}$$

The two dimensional system is reduced to one dimensional system. However by setting $dx_1/dt = 0$ changes the character of the mathematical problem. Setting $dx_1/dt = 0$ implies that x_1 is a constant k, but then the equation $k = \dfrac{rc}{k_n + c}$ implies that c must be a constant, too. Hence $dc/dt = 0$. Then $-\dfrac{K_{\max} c}{k_n + c}$=0, meaning $c = 0$. In other words, above derivation can only be right if there is no external nutrient molecule.

One way to justify these derivations is as follows. Under appropriate conditions, c changes more slowly than x_1. So as far as x_1 is concerned, it may be assumed that $c(t)$ is constant, say $c(t) = \bar{c}$. Then, the equation for x_1 becomes a linear equation. Its solution converges to its steady state, which is given by (33) with $c = \bar{c}$) obtained by setting $dx_1/dt = 0$. Now as c changes, x_1 "catches up" very fast so that this formula is always (approximately) valid. From the point of view of c, the variable x_1 is always catching up with ite expression given by (33). Thus as far as its slow motion is concerned, c evolves according to (34). An exception will be at the start of the whole process, when $c(0)$ is initially far from its steady state value.

Example 2.16. A more complicated example.

For an enzyme with n protomers, the time evolution of the metabolites and of the

free or complexed enzyme forms is governed by the following differential equations:

$$\begin{aligned}
\frac{dR_0}{dt} =& - k_1R_0 + k_2T_0 - na_2PR_0 + d_2R_{01} - na_1SR_0 + (d+k)R_{10}\\
&\dots\\
\frac{dR_{0n}}{dt} =& a_2PR_{0(n-1)} - nd_2R_{0n} - na_1SR_{0n} + (d_1+k)R_{1n}\\
&\dots\\
\frac{dR_{nn}}{dt} =& a_1SR_{(n-1)n} - n(d_1+k)R_{nn}\\
\frac{dT_0}{dt} =& k_1R_0 - k_2T_0 - na'ST_0 + (d'+k')T_1\\
&\dots\\
\frac{dS}{dt} =& \nu_i - na_1S\Sigma_0 - (n-1)a_1S\Sigma_1 - ... - a_1S\Sigma_{n-1} + d_1\Sigma_1 + 2d_1\Sigma_2 + ...\\
& nd_1\Sigma_n - na'ST_0 - (n-1)a'ST_1 - ...\\
& - a'ST_{n-1} + d'T_1 + 2d'T_2 + ... + nd'T_n\\
\frac{dP}{dt} =& - na_2PR_0 - (n-1)a_2PR_{01} - ... - a_2PR_{0(n-1)} + d_2R_{01} + 2d_2R_{02} + ...\\
=& nd_2R_{0n} + k\Sigma_1 + 2k\Sigma_2 + ... + nk\Sigma_n + k'T_1 + 2k'T_2 + ...\\
& + nk'T_n - k_sP
\end{aligned}$$

together with the conservation relations:

$$R_0 + R_{ij} + T_0 + T_i = D_0 \quad (i,j,=1,...)$$

where S and P denote the concentrations of substrate and product, while R_{ij} are the concentration of enzyme form in the R state carrying i molecules of substrate bound to the catalytic site and j molecules of product bound to the regulatory site; T_i denotes the concentration of enzyme in the T state carrying i molecules of S. The sum of R forms carrying i molecules of substrate is

$$\Sigma_i = \sum_{j=0}^{n} R_{ij}, \quad i = 0, ..., n$$

The other constants are kinetic constants. See [6] for details.

If the concentration of the enzyme is known, which is much smaller than those of the substrate and product, the enzyme forms evolve much more rapidly than the metabolites. Then a quasi-steady state approximation can be made for the enzyme, i.e.

$$\frac{dR_0}{dt} = 0, \ \frac{dR_{ij}}{dt} = 0, \ \frac{dT}{dt} = 0$$

yield two ordinary differential equations. Normally some normalizations take place too, as did in the Chemostat example.

The above discussed system is shown in the following figure.

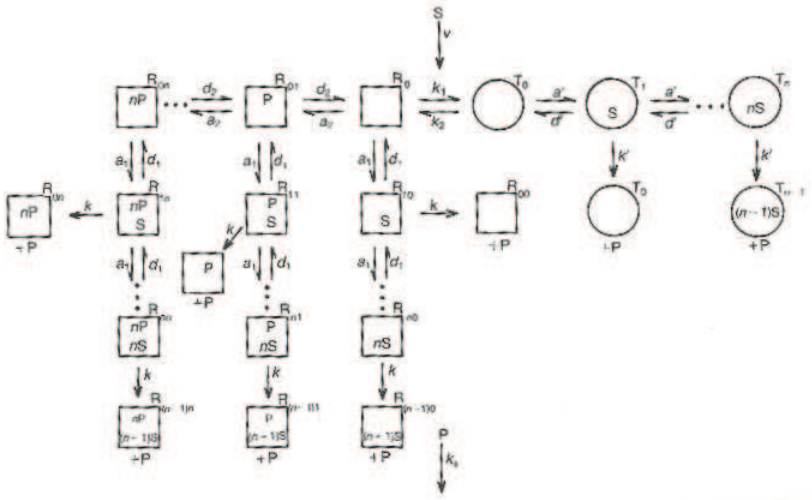

Figure 6: Allosteric model for glycolytic oscillations. The enzyme is formed by n subunits existing in the states R and T. The substrate (S), injected at a constant rate, binds to the two forms of the enzyme with different affinities. The complexes thus formed in the two states decompose with different rates to yield the product (P). The latter binds in an exclusive manner to the the most active, R, form of the enzyme, and disappears from the reaction medium in an apparent first-order reaction (Goldbeter Lefever, 1972; Venieratos Goldbeter, 1979; Goldbeter, 1980). [16]

2.5 Stability analysis of limit cycles

In mathematics, in the area of dynamical systems, a limit cycle on a plane or a two dimensional manifold is a closed trajectory in the phase space having the property that at least one other trajectory spirals into it either as time approaches infinity or as time approaches negative infinity. Such behaviour is exhibited in some nonlinear systems. In the case where all the neighbouring trajectories approaches infinity, it is called a stable or attractive limit cycle. If instead all neighbouring trajectories approach it as time approaches negative infinity, it is unstable or non attractive limit cycle.

The limit cycle imply self sustained oscillations. Any small perturbation from the closed trajectory would cause the system to return to the limit cycle, making the system stick to the limit cycle. An example of a limit cycle is an undamped pendulum which have a closed circle orbit equal to the amplitude of the pendulum's swing.

3 Center manifold theorem

We saw in section 2 how to use linearization to study stability of steady states. We also saw that it fails when the jacobian matrix evaluated at the steady state, has some eigenvalues with zero real parts and no eigenvalues with positive real parts. In this case the center manifold theorem provides a powerful tool in dynamical systems that

reduces the dimension of a system to enable calculations easier.

Recall that for the linear system $\dot{x} = Ax$ the corresponding invariant subspaces $\mathcal{E}^u$, $\mathcal{E}^s$ and $\mathcal{E}^c$ have the characterizations

$$\mathcal{E}^u = \{x \in \mathbb{R}^n : \exists\ c > 0 \text{ such that } \lim_{t \to -\infty} |e^{-ct} e^{At} x| = 0\}$$

$$\mathcal{E}^s = \{x \in \mathbb{R}^n : \exists\ c > 0 \text{ such that } \lim_{t \to +\infty} |e^{ct} e^{At} x| = 0\}$$

and

$$\mathcal{E}^c = \{x \in \mathbb{R}^n : \forall c > 0 \lim_{t \to -\infty} |e^{ct} e^{At} x| = 0 \text{ and } \lim_{t \to +\infty} |e^{-ct} e^{At} x| = 0\}$$

The stable manifold theorem tells that for the nonlinear system $\dot{x} = f(x)$ with $f(0) = 0$, the stable manifold $\mathcal{E}^s(0)$ and the unstable manifold $\mathcal{E}^u(0)$ have characterizations similar to $\mathcal{E}^s$ and $\mathcal{E}^u$, respectively:

$$\mathcal{E}^s = \{x \in \mathbb{R}^n : \exists\ c > 0 \text{ such that } \lim_{t \to -\infty} |e^{ct} \varphi(t, x)| = 0\}$$

and

$$\mathcal{E}^u = \{x \in \mathbb{R}^n : \exists\ c > 0 \text{ such that } \lim_{t \to -\infty} |e^{-ct} \varphi(t, x)| = 0\}$$

where φ is the flow generated by the nonlinear system. Now a center manifold similar to $\mathcal{E}^c$ of the linear system is defined.

Let $A = Df(0)$. A center manifold $W^c(0)$ of the equilibrium point 0 of the system $\dot{x} = f(x)$ is an invariant manifold whose dimension is equal to the dimension of the invariant subspace $\mathcal{E}^c$ and which is tangent to $\mathcal{E}^c$ at the origin.

Theorem 3.1. *A local center manifold exists.*

For the proof of existence of a center manifold please refer to [7].

Note that the stable manifold and the unstable manifold are unique while center manifolds may not be unique. For example

Example 3.2. Consider the system

$$\dot{x} = x^2, \dot{y} = -y$$

By considering the linear part we get

$$A = \begin{pmatrix} 0 & 0 \\ 0 & -1 \end{pmatrix}$$

It is obvious that the x-axis is a center manifold, but it is not the only center manifold. Now solve this system by eliminating t:

$$\frac{dy}{dx} = \frac{-y}{x^2}$$

It has a solution

$$y = ce^{1/x}$$

So

$$\{(x, y) \in \mathbb{R}^2 : x < 0 \text{ and } y = ce^{1/x}\} \cup \{(x, 0) \in \mathbb{R}^2 : x \geq 0\}$$

is also a center manifold.

This example raised two questions

(i) How is the center manifold calculated in general?

(ii) If the center manifold is not unique, what does the center manifold calculation actually calculate?

The following construction answers the first question.

For simplicity it is assumed that the nonlinear system is already transformed to

$$\begin{cases} \dot{x} = Ax + F(x, y) \\ \dot{y} = By + G(x, y) \end{cases} \tag{35}$$

where $x \in \mathcal{E}^c$, $y \in \mathcal{E}^s \oplus \mathcal{E}^u$, the eigenvalues of A all have zero real part, all of the eigenvalues of B have nonzero real part, and F and G are higher order terms.

It is assumed that $y = h(x)$ is an invariant center manifold of the nonlinear system. Then

$$\dot{y} = Dh(x)\dot{x}.$$

By (35)

$$Dh(Ax + F(x, h(x))) = Dh(x)\dot{x} = \dot{y} = Bh(x) + G(x, h(x))$$

Thus, if an operator $\mathcal{M}$ is defined by the formula

$$(\mathcal{M}\varphi)(x) := D\varphi(x)(Ax + F(x, \varphi(x))) - B\varphi(x) - G(x, \varphi(x))$$

the function h whose graph is the center manifold is a solution of the equation $\mathcal{M}h = 0$. This is the condition every center manifold should meet. It seems like finding h is much harder than the original problem of establishing stability of the origin. However something is gained in this complicated calculation.

Theorem 3.3 (Approximation Theorem)**.** *Let $\varphi : \mathbb{R}^c \to \mathbb{R}^s$ be a C^1 map with $\varphi(0) = 0, D\varphi(0) = 0$. If $\mathcal{M}(\varphi(x)) = \mathcal{O}(|x|^q)$ as $x \to 0$ (for $q > 1$), then*

$$|h(x) - \varphi(x)| = \mathcal{O}(|x|^q) \quad \text{as } x \to 0$$

This theorem allows to use a power series to approximate the center manifold to an arbitrary degree of accuracy. This answers the second question raised above.

With $y = h(x)$ the dynamics of the nonlinear system to the center manifold can be reduced. It is governed by

$$\dot{x} = Ax + F(x, h(x)) \tag{36}$$

Now we can state the following theorem:

Theorem 3.4. *Assume all of the conditions in the previous theorem, then the zero solution of $\dot{x} = f(x)$ is stable, asymptotically stable, or unstable if the zero solution of* (36) *is stable, asymptotically stable or unstable respectively.*

Example 3.5. Consider the four dimensional system

$$\begin{aligned} \dot{x}_1 &= -x_2 + x_1(1 - y)y \\ \dot{x}_2 &= x_1 + x_2(1 - y)y \\ \dot{x}_3 &= -x_3^3(1 + y) \\ \dot{y} &= -y + x_1^2 + x_2^2 + 2(1 - y)y^2 \end{aligned}$$

Clearly 0 is an equilibrium point. But conclusion about stability from the Lyapunov linearization theorem can't be drawn, since

$$A = \begin{pmatrix} 0 & -1 & 0 & 0 \\ 1 & 0 & 0 & 0 \\ 0 & 0 & 0 & 0 \\ 0 & 0 & 0 & 1 \end{pmatrix}$$

So the next step would be to reduce the system by studying the flow on a center manifold. Let

$$h(x_1, x_2, x_3) = x_1^2 + x_2^2$$

It is to be checked that the graph condition ($\mathcal{M}h = 0$) is valid.

$$\begin{aligned} Dh(x) \cdot x =& 2x_1\dot{x}_1 + 2x_2\dot{x}_2 \\ =& 2(1 - x_1^2 - x_2^2)(x_1^2 + x_2^2)^2 \\ \dot{y} =& -y + x_1 + x_2^2 + 2(1-y)y^2 \\ =& 2(1 - x_1^2 - x_2^2)(x_1^2 + x_2^2)^2 \end{aligned}$$

The flow on this manifold is governed by

$$\begin{aligned} \dot{x}_1 &= -x_2 + x_1(1 - x_1^2 + x_2^2)(x_1^2 + x_2^2) \\ \dot{x}_2 &= x_1 + x_2(1 - x_1^2 + x_2^2)(x_1^2 + x_2^2) \\ \dot{x}_3 &= -x_3^3(1 - x_1^2 + x_2^2) \end{aligned} \tag{37}$$

Note that the first two equations are decoupled from the last one. Now the stability of the origin should be analyzed. Make polar coordinate change: $x_1 = r\cos\theta$, $x_2 = r\sin\theta$. Then the above system reduces to

$$\begin{aligned} \dot{r} &= r^3(1 - r^2) \\ \dot{\theta} &= 1 \\ \dot{x}_3 &= -x_3^3(1 - r^2) \end{aligned}$$

It can be shown that there is a stable limit cycle $r = 1$ because for $V(r) = -r^4/4 + r^6/6 + 1/12$, $V(1) = 0$, $V > 0$ in the neighborhood of $r = 1$, and

$$\dot{V} = -r^6(1 - r^2)^2 < 0$$

Hence, the origin is unstable and the system (37) has a stable limit cycle defined by $\mathcal{C}_3 = (\cos t, \sin t, 0)$. Together with the center manifold theorem it implies that the original system should have a stable limit cycle defined by $\mathcal{C}_4 = (\cos t, \sin t, 0, 0)$.
Now proof on above mentioned claims are given.

Consider the function $V(x_1, x_2, x_3) = -r^4/4 + r^6/6 + 1/12 + x_3^2$ with $r = \sqrt{x_1^2 + x_2^2}$. Clearly, $V(\mathcal{C}_3) = 0$ and $V > 0$ in the neighborhood of $\mathcal{C}_3$. Moreover

$$\dot{V} = -(r^6(1 - r^2)^2 - 2x_3^4(1 + r^2) < 0$$

in the neighborhood of $\mathcal{C}_3$. Hence $\mathcal{C}_3$ is a stable limit cycle of (37).

It is natural to think that a similar argument will lead to the claim $\mathcal{C}_4$ is a stable limit cycle for the original system by considering $V = (x_1, x_2, x_3, y) = -r^4/4 + r^6/6 + 1/12 + x_3^2 + y^2$. Nevertheless

$$\dot{V} = -(1-r^2)r^4(1-y)y - 2x_3^4(1+y) - 2y^2 + 2yr^2 + 4(1-y)y^3$$

whose sign is not at all clear. So direct methods does not seem to work here. This might tell us that the system does not always stay on the limit cycle. It might take some time to approach the limit cycle then if it is close enough then it stays on the limit cycle. To see this, the proof is divided into two steps. Firstly it is shown that the trajectory eventually converge to the center manifold globally, the above given V on the center manifold is used to show that the limit cycle is stable.

Let $U = (y - x_1^2 - x_2^2)^2$. Obviously, $U = 0$ for $y = x_1^2 + x_2^2$ and $U > 0$ otherwise. Note that

$$\dot{U} = -2(y - x_1^2 + x_2^2)^2(y^2 + (y-1)^2)$$

and therefore $\dot{U} < 0$ for $y \neq x_1^2 + x_2^2$ and 0 otherwise. So trajectories eventually converge to the center manifold. Note that it is just proved global convergence (different than the local construction).

It can be shown that $\dot{V} < 0$ on the neighborhood of the center manifold $y = x_1^2 + x_2^2 = r = 2$, i.e., $y = x_1^2 + x_2^2 + \epsilon = r^2 + \epsilon$.

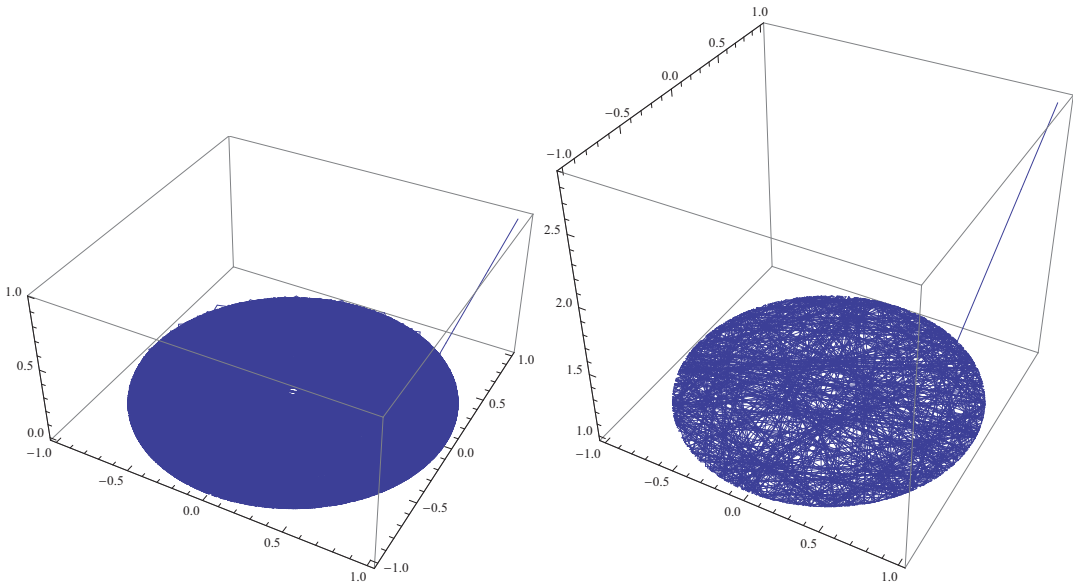

Figure 7: Figures for the above example

These are the plots for (x_1, x_2, x_3) and (x_1, x_2, y) which shows that the trajectories converge to the center manifold $x_1^2 + x_2^2 = 1$.

Note that we have read Lyapunov- type of functions in our analysis. It is not always appreciated in biological models as explained earlier. However, the theorem is useful to prove stability of limit cycle.

In next section we will give an example on center manifold reduction to Hopf bifurcation.

4 Bifurcation theory

Bifurcation theory is the mathematical study of changes in the qualitative or topological structure of a given family. Examples of such families are the integral curves of a family of vector fields or, the solutions of a family of differential equations. Most commonly applied to the mathematical study of dynamical systems, a bifurcation occurs when a small smooth change made to the parameter values (the bifurcation parameters) of a system causes a sudden 'qualitative' or topological change in its behaviour. Bifurcations occur in both continuous systems (described by ODEs, DDEs or PDEs), and discrete systems (described by maps).

The dynamics of one-dimensional systems is very limited (all solutions either settle down to a steady equilibrium or head off to one of $\pm\infty$). They can have an interesting dependence on parameters. In particular, the qualitative structure of the flow can change as parameters are varied. These qualitative changes in the dynamics are called bifurcations and the parameter values at which they occur are called bifurcation points. Bifurcations provide models of transitions and instabilities as some control parameters are varied.

4.1 Types of bifurcation

It is useful to divide bifurcations into two principal classes:

1. **Local Bifurcations**

   Local bifurcations, which can be analysed entirely through changes in the local stability properties of equilibria, periodic orbits or other invariant sets as parameters cross through critical thresholds. A local bifurcation occurs when a parameter change causes the stability of an equilibrium (or fixed point) to change. In continuous systems, this corresponds to the real part of an eigenvalue of an equilibrium point passing through zero. In discrete systems (those described by maps rather than ODEs), this corresponds to a fixed point having a Floquet multiplier with modulus equal to one. In both cases, the equilibrium is "non-hyperbolic" at the bifurcation point. The topological changes in the phase portrait of the system can be confined to arbitrarily small neighbourhoods of the bifurcating fixed points by moving the bifurcation parameter close to the bifurcation point (hence 'local').

   Examples of local bifurcations include:

   (a) Saddle-node (fold) bifurcation

   (b) Transcritical bifurcation

   (c) Pitchfork bifurcation

   (d) Period-doubling (flip) bifurcation

   (e) Hopf bifurcation

(f) Neimark (secondary Hopf) bifurcation

2. **Global Bifurcations**

   Global bifurcations occur when 'larger' invariant sets of the system, such as periodic orbits, collide with each other, or with equilibria of the system. They cannot be detected purely by a stability analysis of the equilibria (fixed points). This causes changes in the topology of the trajectories in the phase space which cannot be confined to a small neighbourhood, as is the case with local bifurcations. In fact, the changes in topology extend out to an arbitrarily large distance (hence 'global').

   Examples of global bifurcations include:

   (a) Homoclinic bifurcation in which a limit cycle collides with a saddle point.

   (b) Heteroclinic bifurcation in which a limit cycle collides with two or more saddle points.

   (c) Infinite-period bifurcation in which a stable node and saddle point simultaneously occur on a limit cycle.

   (d) Blue sky catastrophe in which a limit cycle collides with a nonhyperbolic cycle.

   Global bifurcations can also involve more complicated sets such as chaotic attractors.

4.2 Saddle-node bifurcation

A saddle-node bifurcation is a collision and disappearance of two equilibria in dynamical systems. In systems generated by autonomous ODEs, this occurs when the critical equilibrium has one zero eigenvalue. In other words if the phase plane is one-dimensional, one of the equilibrium points is unstable (the saddle), while the other is stable (the node). This phenomenon is also called fold or limit point bifurcation.[3]

For example consider the system

$$x' = \alpha + x^2$$

where α is a real valued parameter. The fixed points of the system are given by

$$\alpha + x^2 = 0 \Rightarrow x^2 = -\alpha$$

Three possibilities can be observed here.

1. $\alpha < 0$: in this case $-\alpha$ is positive, means square root can be taken. Thus there are two distinct fixed points

   $$x^* = \pm\sqrt{\alpha}$$

   The phase portraits do not change qualitatively as α changes in this range. The fixed point at $-\sqrt{-\alpha}$ is always stable and the fixed point at $\sqrt{-\alpha}$ is unstable.

2. $\alpha = 0$: There is only one fixed point

$$x^* = 0$$

which is semi-stable.

3. $\alpha > 0$: in this case there are no fixed points, and the value of x increases forever.

4.3 Hopf bifurcation

In bifurcation theory a Hopf or Andronov-Hopf bifurcation is a local bifurcation in which a fixed point of a dynamical system loses stability as a pair of complex conjugate eigenvalues of the linearization around the fixed point cross the imaginary axis of the complex plane. More rigorously, the existence of a limit cycle close to such a steady-state is established by the Hopf bifurcation theorem.

Theorem 4.1. ***Hopf(Andronov-Hopf) Bifurcation Theorem.***
Suppose $x' = f(x, y)$ has an isolated steady state at x_1. Let $\frac{\partial(x')}{\partial(y)} = A(y)$ is Jacobian of f at x_1. Suppose that $A(y)$ has a pair of complex conjugate eigenvalues $\lambda_{1,2} = \alpha(y) \pm i\beta(y)$. Suppose that the following conditions hold for $y = y_0$

1. *$\alpha(y_0) = 0$.*
2. *$\beta(y_0) = \beta_0 > 0$.*
3. *$\gamma \equiv \frac{\partial(\alpha(y))}{\partial(y)} \mid_{y=y_0} \neq 0$, i.e. transversality (strict-crossing)*
4. *$A(y_0)$ has no other eigenvalues with zero real part.*

then the system contains an isolated limit cycle for $\mid y - y_0 \mid$ small for either $y > y_0$ or for $y < y_0$. The magnitude of the limit-cycle is proportional to $\sqrt{\mid y - y_0 \mid}$ and the frequency is close to β_0. If $\gamma > 0$ and the limit cycle exists for $y > y_0$ or if $\gamma < 0$ and the limit cycle exists for $y < y_0$ then it is stable, otherwise it is unstable.

Proof. see e.g., Guckenheimer and Holmes [4] □

Hopf bifurcation points are categorized as being either supercritical or subcritical, depending on whether the limit cycle born at the steady-state is stable or unstable, respectively. Whether a specific Hopf point is sub- or supercritical can be determined based on the first Lyapunov coefficient, e.g.(Kuznetsov, 1998). According to the Hopf theorem, the birth of a limit cycle is hence associated with loss of stability of a steady-state solution. This implies again that a limit cycle usually will coexist with an unstable steady-state. The latter always holds when the Hopf is supercritical and there are no subsequent multiple limit cycle bifurcations of the limit cycle. However in the case of subcritical Hopf points will there usually be an unstable steady-state coexisting with the limit cycle and the two are connected through a Hopf point. The reason in this latter case is that the unstable cycle born at the Hopf point will have to bifurcate to generate a stable limit cycle, and the branch of stable limit cycles will then usually extend over the branch of unstable steady-states. For systems in which an unstable steady-state coexists with the limit cycle, a perturbation that translates the steady-state into a Hopf bifurcation point will correspond to removal of a limit cycle.

If the induced Hopf is supercritical, the stable limit cycle will disappear. However, also for cases in which the induced Hopf is subcritical will the perturbation result in a qualitative change of the network behavior in the sense that the limit cycle will coexist with a stable steady-state after the perturbation and hence at best be locally stable. Indeed, it is common when considering robustness with respect to parameter variations to use the existence of stable steady-states as a criteria in the robustness analysis, e.g., (Kim et al., 2006;Leloup and Goldbeter, 2004).

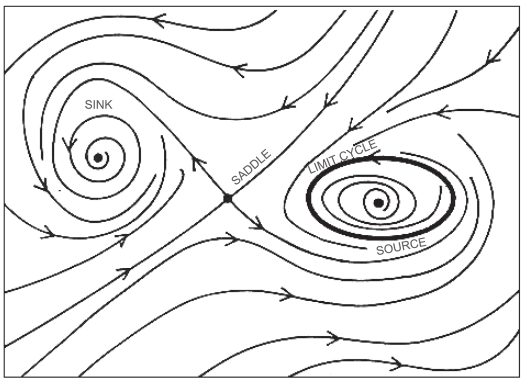

Source: Stewart (1989)

Figure 8: Figure showing the difference between the certain bifurcation conditions

Example 4.2. Investigating the effect of changing the parameter α on the dynamical system

$$\dot{x} = \alpha x - y - (x + \frac{3}{2}y)(x^2 + y^2) \tag{38}$$

$$\dot{y} = x + \alpha y + (\frac{3}{2}x - y)(x^2 + y^2) \tag{39}$$

It can be shown that the polar form of the system is

$$\dot{r} = \alpha r - r^3 \tag{40}$$

$$\dot{\theta} = 1 + \frac{3}{2}r^2 \tag{41}$$

from which it is clear that there is a single equilibrium point at the origin. The first polar equation can be written as

$$\dot{r} = r(\sqrt{\alpha} + r)(\sqrt{\alpha} - r), \alpha > 0 \tag{42}$$

Clearly there is a limit cycle of radius $\sqrt{\alpha}$ in this case. The origin is unstable since for small r

$$\dot{r} \simeq \alpha r \tag{43}$$

which is positive. If $\alpha \leq 0$ then $\dot{r} < 0$ and the origin is globally asymptotically stable. This behaviour is illustrated in the figure for the cases $\alpha = -4$ and $\alpha = 4$ respectively.

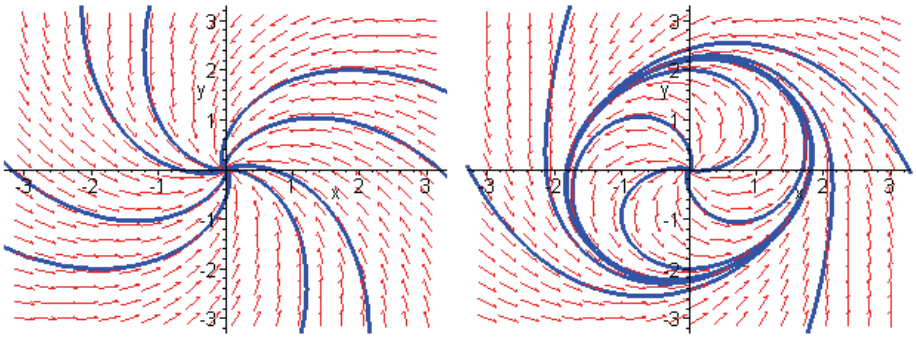

Figure 9: For $\alpha = -4$ (stable focus) and for $\alpha = 4$ (unstable focus but stable limit cycle)

It can be seen from the figures that as the parameter α passes through zero from negative to positive, a stable focus gives way to an unstable focus surrounded by a stable limit cycle whose radius increases with $\sqrt{\alpha}$.

Now we show how to use center manifold reduction.

Example 4.3. Consider

$$\dot{x_1} = x_2 \tag{44}$$

$$\dot{x_2} = -x_1 - 2ax_2 - x_1x_3 \tag{45}$$

$$\dot{x_3} = -x_3 + x_1^2 \tag{46}$$

Put this system in the form $\dot{x} = A(a)x + f(x)$
Here

$$\dot{x} = \begin{pmatrix} \dot{x_1} \\ \dot{x_2} \\ \dot{x_3} \end{pmatrix}, A(a) = \begin{pmatrix} 0 & 1 & 0 \\ -1 & 2a & 0 \\ 0 & 0 & -1 \end{pmatrix}, f(x) = \begin{pmatrix} 0 \\ -x_1x_3 \\ x_1^2 \end{pmatrix}$$

The eigenvalues of $A(a)$ are $+i, -i, -1$ when $a = 0$.
This indicates the possibility of a Hopf bifurcation. Now we follow the scheme provided in [3] to compute the first Lyapunov coefficient.
(i) Find eigenvectors of A and $A^\star$ (the adjoint of A)

$$u = \begin{pmatrix} i \\ 1 \\ 0 \end{pmatrix} = v, Au = iu, A^\star v = -iv$$

(ii) For normalization purposes, let $v = \frac{1}{2}u$ Then we have $\langle v, u\rangle = 1$. Now check the Hopf crossing condition

$$\gamma'(0) = \langle v, A'(0)u\rangle = \langle \frac{1}{2}\begin{pmatrix} i \\ 1 \\ 0 \end{pmatrix}, \begin{pmatrix} 0 & 0 & 0 \\ 0 & -2 & 0 \\ 0 & 0 & 0 \end{pmatrix}\begin{pmatrix} i \\ 1 \\ 0 \end{pmatrix}\rangle = 1/2 \times \langle \begin{pmatrix} i \\ 1 \\ 0 \end{pmatrix}, \begin{pmatrix} 0 \\ -2 \\ 0 \end{pmatrix}\rangle = -1$$

Since $\gamma'(0) \neq 0$. This implies that there exists a Hopf bifurcation at $\lambda = 0$.
(iii) Compute the first Lyapunov coefficient $l_1(0)$. First we write the system in its

complex normal form

$$\dot{z} = iwz + 1/2(g_{20}z^2 + 2g_{11}z\bar{z} + g_{02}\bar{z}^2) + 1/2g_{21}z^2\bar{z}^2 + ...$$

where

$$g_{20} = \langle v, B(u,u)\rangle, g_{11} = \langle v, B(u,\bar{u})\rangle$$

$$g_{21} = \langle v, C(u,u,\bar{u})\rangle - 2\langle v, B(u, A^{-1}B(u,\bar{u}))\rangle + \langle v, B(\bar{u}, (2iwI-1)^{-1}B(u,u))\rangle + L$$

where

$$L = (1/iw)\langle v, B(u,u)\rangle\langle v, B(u,\bar{u})\rangle - (2/iw)|\langle v, B(u,\bar{u})\rangle|^2 - (1/3iw)|\langle v, B(\bar{u},\bar{u})\rangle|^2$$

And

$$A = A(0)$$

$B(x,x)$ and $C(x,x,x)$ are the second and third order terms respectively. Here we emit the explicit expression of g_{02}, since it is not used in our calculation. As $f(x)$ has only quadratic terms so we see that $C(x,x,x) = 0$, and

$$B(x,x) = 2f(x,x) = \begin{pmatrix} 0 \\ -2x_1x_3 \\ 2x_1^2 \end{pmatrix} \Longrightarrow B(x,y) = \begin{pmatrix} 0 \\ -2x_1y_3 \\ 2x_1y_1 \end{pmatrix}$$

By definition the first Lyapunov coefficient is defined as the quantity

$$l_1(0) = (1/2w^2)\mathrm{Re}(ig_{20}g_{11} + wg_{21})$$

In this example $w = 1$. Now both g_{20} and g_{11} are real, $\mathrm{Re}(ig_{20}g_{11}) = 0$, and the last three terms in g_{21} are imaginary, so $l_1(0)$ can be rewritten in the following way

$$l_1(0) = (1/2w)\mathrm{Re}(g_{21}) = (1/2w)\mathrm{Re}[\langle v, C(u,u,\bar{u})\rangle - 2\langle v, B(u, A^{-1}B(u,\bar{u}),\rangle + L_1]$$

Where

$$L_1 = \langle v, B(\bar{u}, (2iwI-1)^{-1}B(u,u))\rangle$$

Now consider the second term in $l_1(0)$. After putting values and simplifying

$$-2\langle v, B(u, A^{-1}B(u,\bar{u})\rangle = 4i$$

So the second term in $l_1(0)$ is imaginary, thus it does not contribute to $l_1(0)$. The last term becomes

$$\langle v, B(\bar{u}, (2iwI-1)^{-1}B(u,u))\rangle = (4/10)(2+i)$$

Using these values we obtain

$$l_1(0) = (1/2)\mathrm{Re}(0 + 4i + (4/5) + (2/5)i) = 2/5 \text{ that is } l_1(0) > 0$$

By the following theorem the Hopf bifurcation is supercritical, i.e the limit cycle is stable.

Theorem 4.4 (Stability of Hopf bifurcation [3]). *Consider the equation*

$$\dot{x} = A(a)x + f(x, a)$$

where $x \in R^n$, $a \in R$ *with* $f(x, a) \in C^k, k \geq 2$, $f(0, 0) = Df(0, 0) = 0$. *Let its center manifold reduction have the form*

$$\dot{z} = iwz + 1/2(g_{20}z^2 + 2g_{11}z\bar{z} + g_{02}\bar{z}^2) + 1/2g_{21}z^2\bar{z}^2 + ...$$

then the Hopf bifurcation is subcritical iff $l_1(0) > 0$ *and supercritical iff* $l_1(0) < 0$.

We close this section by the following remarks:

1. The Lyapunov coefficient $l_1(0)$ is not unique, since different normalizations will result in a different quantity, see [3]. However the sign of $l_1(0)$ is preserved.
2. When $l_1(0) = 0$, the system undergoes a further bifurcation, which is called Bautin bifurcation. To study stability of Bautin bifurcation we need the second Lyapunov coefficient. An example for existance of Bautin bifurcation is the model of 3-dimensional circadian rhythms [10].

4.4 A discussion on bifurcation of the five dimensional model of circadian rhythm

The five variable model for circadian rhythms is given in the previous sections. Here we solve the five variable model numerically. Parameter values used to solve the system are given in the following table.

Parameter	**Value**	**Parameter**	**Value**
k_1	1.9	k_2	1.3
V_1	3.2	V_2	1.58
V_3	5	V_4	2.5
K_1	2	K_2	2
K_3	2	K_4	2
K_I	1	v_m	0.65
v_s	0.76	k_m	0.5
k_s	0.38	v_d	0.95
k_d	0.2	n	4

Numerically, in a large domain of parameter values the system reaches a sustained periodic oscillations, instead of stable steady state. The variations in per mRNA and PER are shown in the following figure. This figure also shows the periodic variation in the total amount of PER protein and in the phosphorylated and phosphorylated, cytosolic form of PER. In the whole day(24 Hrs) the phase difference between total PER and per mRNA is shorter.

To solve the given system, as in [8] initial conditions for the variables are assigned in the MATLAB program. These are the sustained oscillations in

PER protein and per mRNA corresponds towards a limit cycle in the (M, P_t) plane. Limit cycle oscillations are normally stable as they are characterized by a unique amplitude and frequency for a given set of parametric values, regardless of initial conditions(Minorsky 1962). The parametric values used here are given in the above given table. The initial condition used here is as follows $M = 1.5, P_0 = P_1 = P_2 = 0.8$, so in this case $P_t = 3.2$.

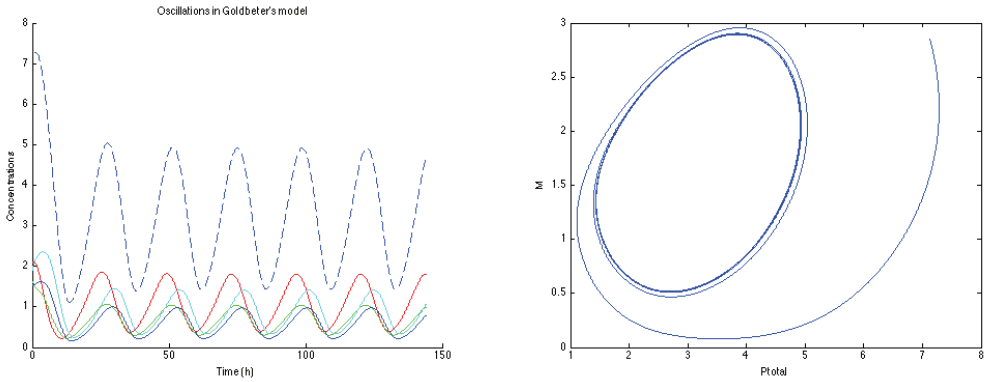

Figure 10: Figures for the solution and phase portrait for given initial conditions

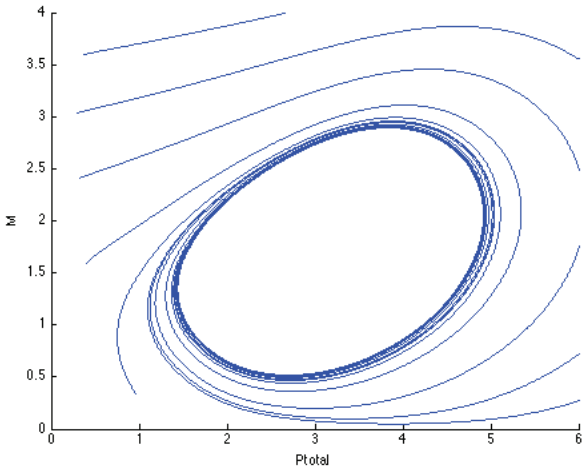

Figure 11: Figure for the limit cycle for different initial points

In the following figure for limit cycles, it can be observed that whatever the starting point is, all the curves end up on the limit cycle.

In present model a parametric family of ordinary differential equations is focussed. By tuning the parameters it is tried to see, how the dynamics is going to change. For this purpose, the given dynamical system is linearized by calculating the Jacobian for a given set of parametric values at a fixed point. By

changing parametric values, it is observed that when real part of an eigen value changes its sign. Change in the sign of real part of eigen value is the indication of bifurcation. Change from positive to negative sign directs towards stability and change from negative to positive directs towards instability.

Firstly focus is on one parameter v_s and to see how the sign is changed of the eigenvalues of the Jacobian. To perform the analysis, all parameters are taken

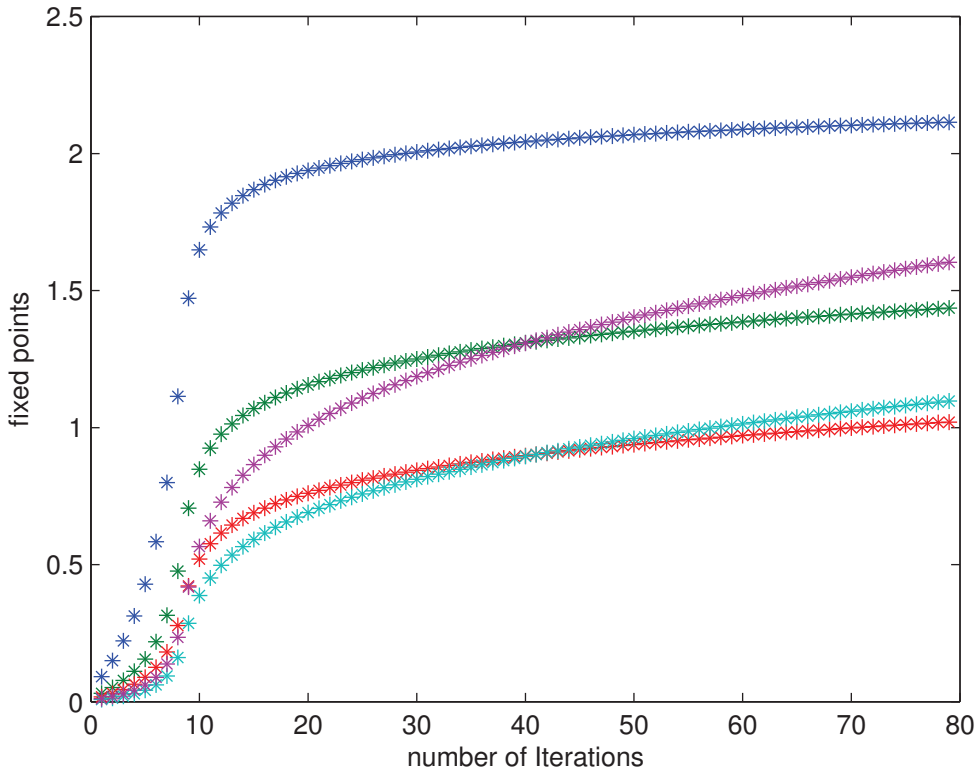

Figure 12: A

as given in the table given above: The range of values of v_s is:

$$v_s = 0.1 : .1/2 : 4;$$

In the plot 'A', it can be observed that by changing the value of v_s, the fixed points moves its position.

Figures B and C are showing the plots between real and imaginary parts of eigen values of Jacobian. It can be seen clearly that at some value of v_s, real parts of two of eigen values are changing the sign from negative to positive. Both eigen values appear as a complex conjugate of each other on the right of y-axis. So, it is the indication of bifurcation. Next section is focussed on to find the exact value of parameter v_s, where the bifurcation is going to occur.

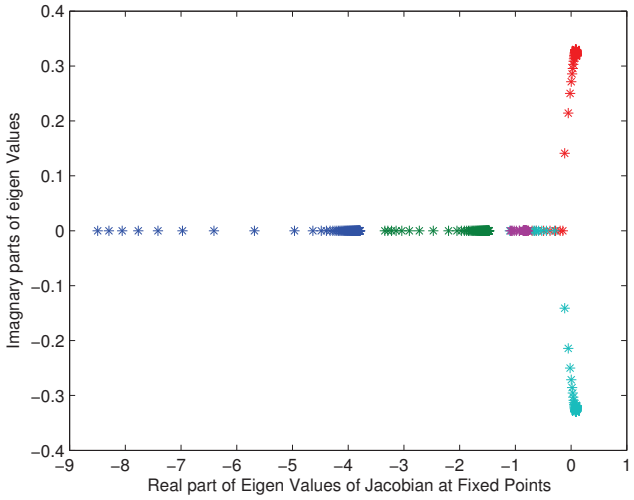

Figure 13: B

For $v_s = 0.637930420865621$, the fixed point and the eigenvalues are

$$\begin{aligned} fixedpoint &= 1.77297321324624 \\ &\quad 0.965038414935763 \\ &\quad 0.606792115161602 \\ &\quad 0.487732569294205 \\ &\quad 0.712839908968454) \\ eigenvalues &= -4.4078869873484 \\ &\quad - 1.92490179477781 \\ &\quad - 5.7848966693308e - 009 + 0.267074602156167i \\ &\quad - 5.7848966693308e - 009 - 0.267074602156167i \\ &\quad - 0.804332460566371 \end{aligned}$$

It is clear that the real parts of pair of complex conjugate eigen-values become almost zero at $v_s = 0.637930420865621$.

Phase portrait are drawn between M and P_{tot} for this value of v_s in the figure D given below

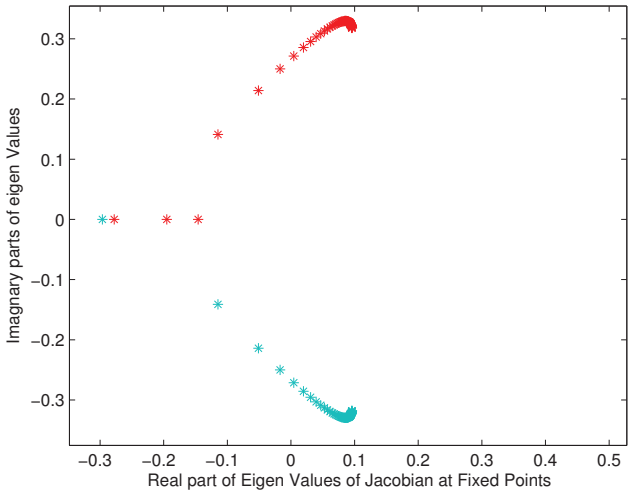

Figure 14: C

Before Bifurcation, $For\ v_s = 0.637930420865621 - 0.1$

The fixed point and the eigenvalues are

$$\begin{aligned} fixedpoint &= 1.6188776969146 \\ &= 0.822100612680711 \\ &= 0.502003810110188 \\ &= 0.367457955009496 \\ &= 0.537053934243986 \\ Eigenvalues &= -4.68746782101408 \\ &= -2.07468612323762 \\ &= -0.0627036866151932 + 0.201460002519662i \\ &= -0.0627036866151932 - 0.201460002519662i \\ &= -0.772776924076349 \end{aligned}$$

Graphs related to these values are given in figure E,

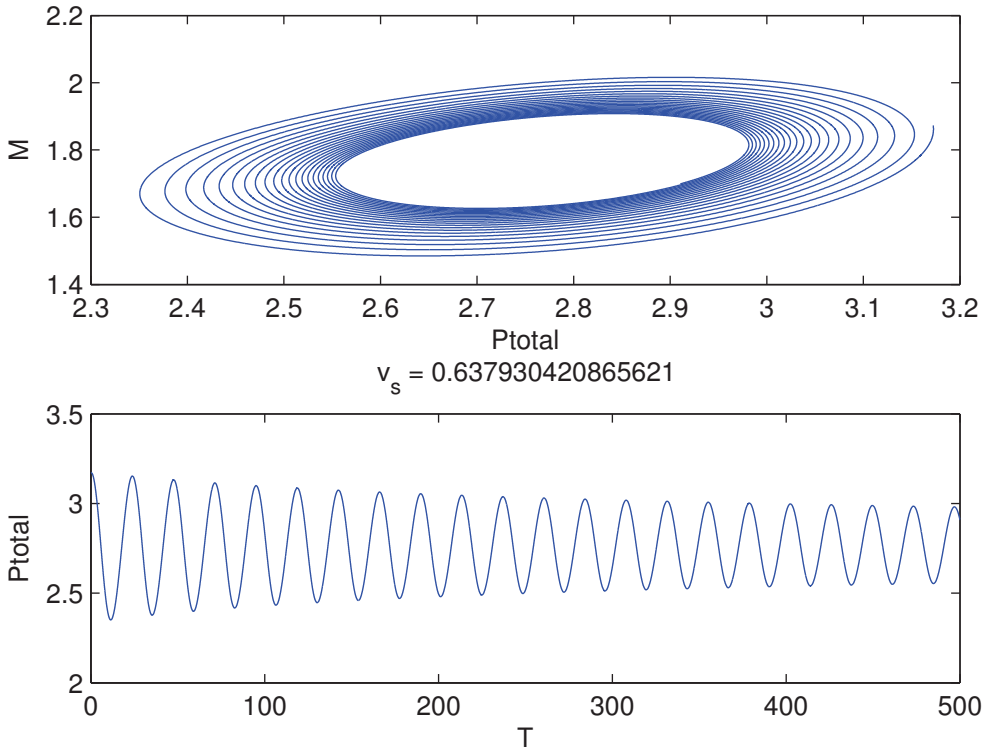

Figure 15: D

After Bifurcation, $For\ v_s = 0.637930420865621 + 0.1$

The fixed point at this value is

$$\begin{aligned} fixedpoint &= 1.8407238201227 \\ &= 1.03740396185673 \\ &= 0.66321110764272 \\ &= 0.558407500924826 \\ &= 0.816134039813207 \end{aligned}$$

The eigenvalues of model linearized around the strictly positive fixed point are

$$\begin{aligned} eigenvalues &= -4.28593147932826 \\ &= -1.84777776455541 \\ &= 0.0284392963379789 + 0.293474694468739i \\ &= 0.0284392963379789 - 0.293474694468739i \\ &= -0.825842286267537 \end{aligned}$$

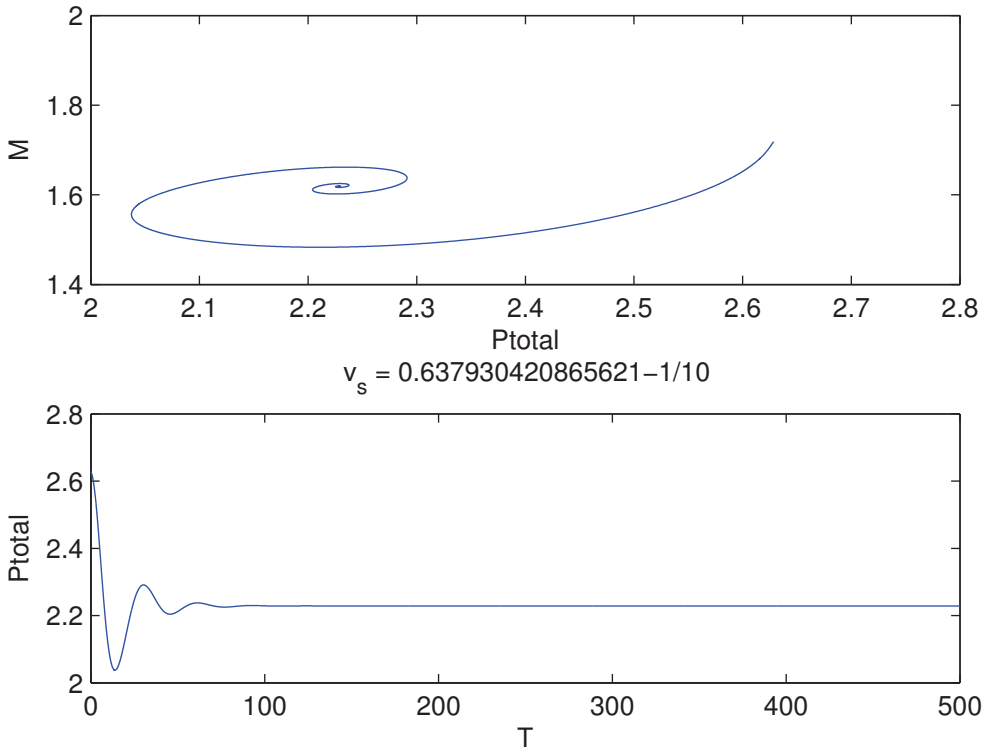

Figure 16: E

Corresponding plots are given in figure F.
These eigenvalues have corresponding eigenvectors as

$$\begin{pmatrix} 0.098 \\ -0.043 \\ 0.26 \\ -0.81 \\ 0.52 \end{pmatrix} \begin{pmatrix} -0.27 \\ -0.18 \\ 0.70 \\ 0.17 \\ -0.61 \end{pmatrix} \begin{pmatrix} 0.78 \\ 0.36 - 0.27i \\ 0.092 - 0.20i \\ -0.017 - 0.22i \\ -0.089 - 0.29i \end{pmatrix} \begin{pmatrix} 0.78 \\ 0.36 + 0.27i \\ 0.092 + 0.20i \\ -0.017 + 0.22i \\ -0.089 + 0.29i \end{pmatrix} \begin{pmatrix} -0.55 \\ 0.57 \\ 0.29 \\ -0.13 \\ -0.52 \end{pmatrix}$$

As it can be seen that three eigenvalues are real, negative and much larger in magnitude than the complex eigenvectors. The next two complex eigenvalues contain a small positive real part. Near the fixed point, the nonlinear dynamics are similar to the dynamics of the corresponding linear syatem.The three negative real eigenvalues are very much larger than the real part of the complex part of eigenvalues. This suggests that any trajectory starting close to two-dimensional plane in the five dimensional space will rapidly converge to it. The real part and the imaginary part of the complex eigenvectors

$$\begin{pmatrix} 0.78 \\ 0.36 \\ 0.092 \\ -0.017 \\ -0.089 \end{pmatrix} \begin{pmatrix} 0 \\ 0.27 \\ 0.20 \\ 0.22 \\ 0.29 \end{pmatrix}$$

span this plane(the plane of linearized oscillation). In the linearized system, trajectories will slowly spiral outward on the plane of linearized oscillation.
As the amplitude of the oscillation increases, nonlinear effects become evident. The manifold of oscillation deforms from the plane of linearized oscillation. Similar to the plane of linearized oscillation, the three negative real eigenvalues and their corresponding eigenvectors determine a three-dimensional stable manifold. Near the fixed point, any trajectory on this three-dimensional manifold will converge to the fixed point of the three-dimensional manifold. For details see [17].

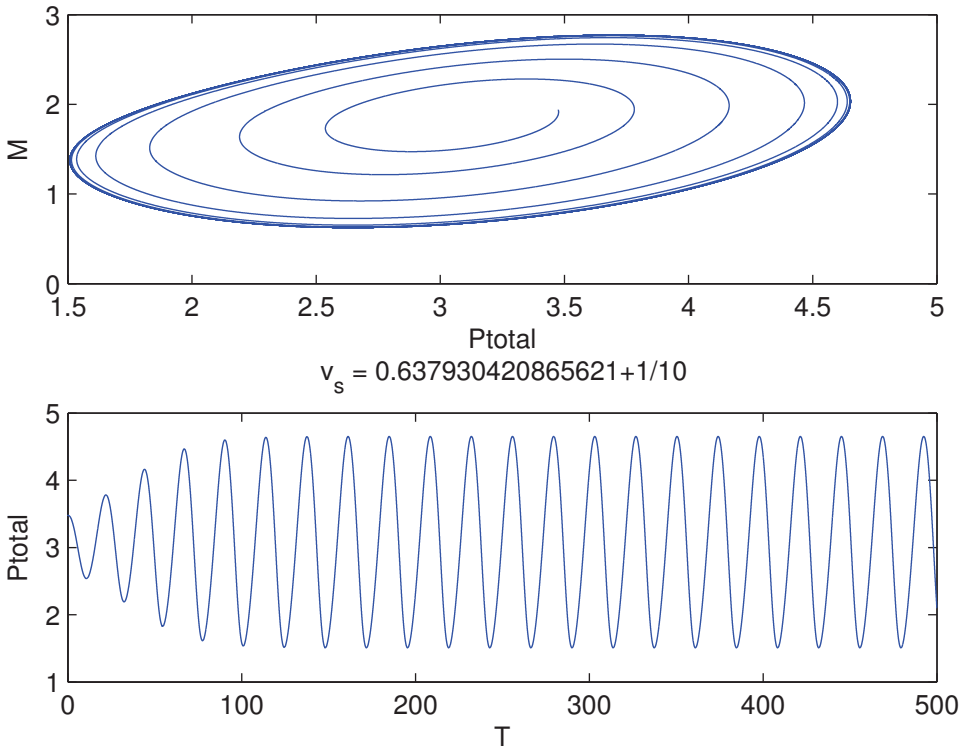

Figure 17: F

Now the critical value is perturbed and integration of the system is started in the neighborhood of fixed point.

Perturbation in the fixed point:

$$\begin{aligned} perturb - fixed - point &= 1.77297321324624 + 0.00001 \\ &= 0.965038414935763 + 0.00001 \\ &= 0.606792115161602 + 0.00001 \\ &= 0.487732569294205 + 0.00001 \\ &= 0.712839908968454 + 0.00001 \end{aligned}$$

From now, in all rest of analysis, perturb-fixed-point will be used as starting point for the integration of the system.
Now for $v_s = 0.637930420865621 - 10^{-4}$, the fixed point and the eigenvalues for the jacobian are

$$\begin{aligned} fixed - point &= 1.77288183697706 \\ &= 0.964945337120554 \\ &= 0.606721071311119 \\ &= 0.487646142576252 \\ &= 0.712713592996062 \\ Eigenvalues &= -4.40805159985492 \\ &= -1.92500049197205 \\ &= -3.87234197764142 \times 10^{-5} + 0.267036917478186i \\ &= -3.87234197764142 \times 10^{-5} - 0.267036917478186i \\ &= -0.804305166680725 \end{aligned}$$

and the corresponding plots are

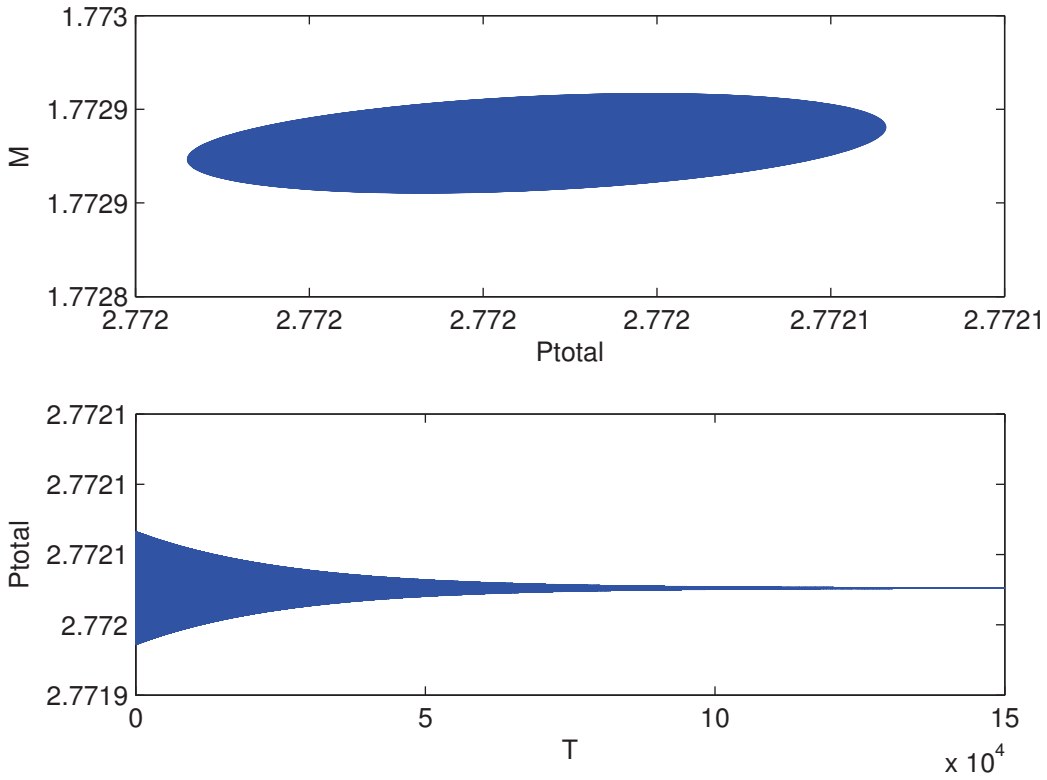

It is clear that if real-parts of complex conjugate of eigen-values are negative, system will converge to fixed point after long integration.
For $v_s = 0.637930420865621 + 10^{-4}$, the fixed point and the eigenvalues of jacobian are

$$\begin{aligned} fixed - point &= 1.77306452179638 \\ &= 0.965131435116119 \\ &= 0.606863118851551 \\ &= 0.487818953664867 \\ &= 0.712966163048652 \\ eigenvalues &= -4.4077224975284 \\ &= -1.92480315698259 \\ &= 3.8683363671169 \times 10^{-5} + 0.26711225493822i \\ &= 3.8683363671169 \times 10^{-5} - 0.26711225493822i \\ &= -0.80435974152151 \end{aligned}$$

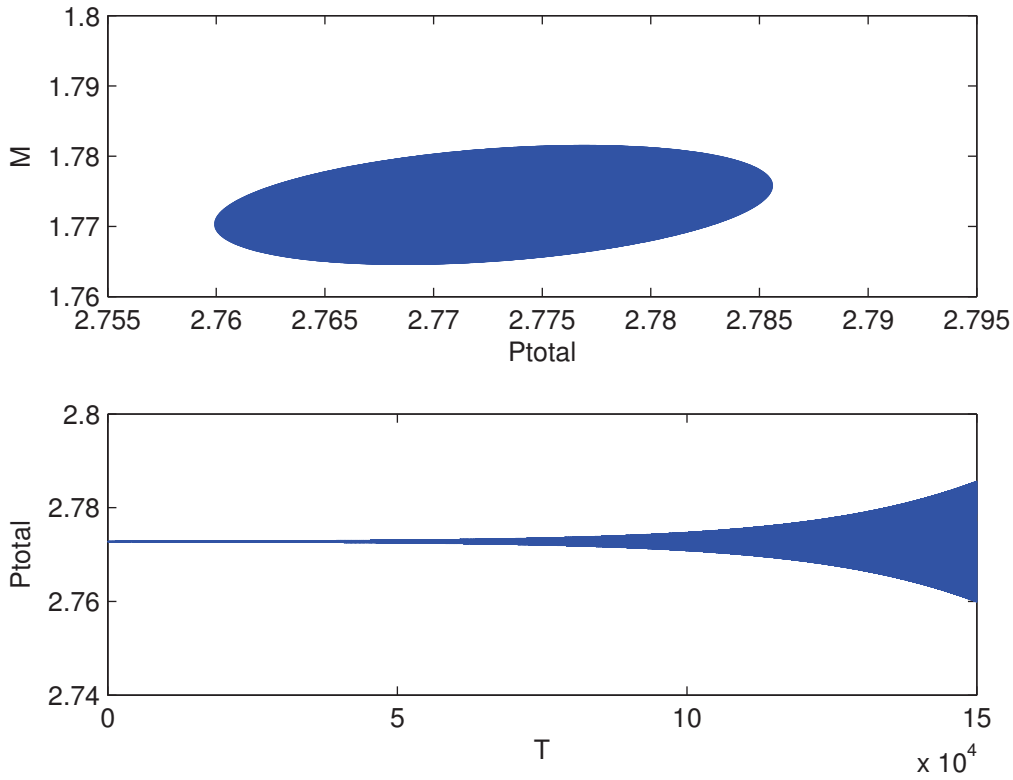

From this it is clearly observed that if real part of complex conjugate pair of eigenvalues are positive, always their exist limit cycle.

4.4.1 Critical value of v_d

From the above analysis, it is seen that two of the eigen-values are complex conjugates and with positive real parts. To find the values of parameter v_d, when the real parts of eigenvalues become zero is of focus here. Actually it is to be observed that when real parts going to change the sign. All the parameters have same values which are given already.

The critical value of v_d is 2.69772513516755 and the corresponding fixed points

and eigenvalues of Jacobian are:

$$\begin{aligned} Fixed-point &= 5.07009317713357 \\ &= 10.6327619854791 \\ &= 1.88562192110702 \\ &= 0.499717539286752 \\ &= 0.730356403572946 \\ Eigenvalues &= -4.67380161140235 \\ &= -0.979450775198323 \\ &= 1.25736128841721e-006 + 0.0913043948282707i \\ &= 1.25736128841721e-006 - 0.091304394828270i \\ &= -0.371146420427092 \end{aligned}$$

And corresponding plots are:

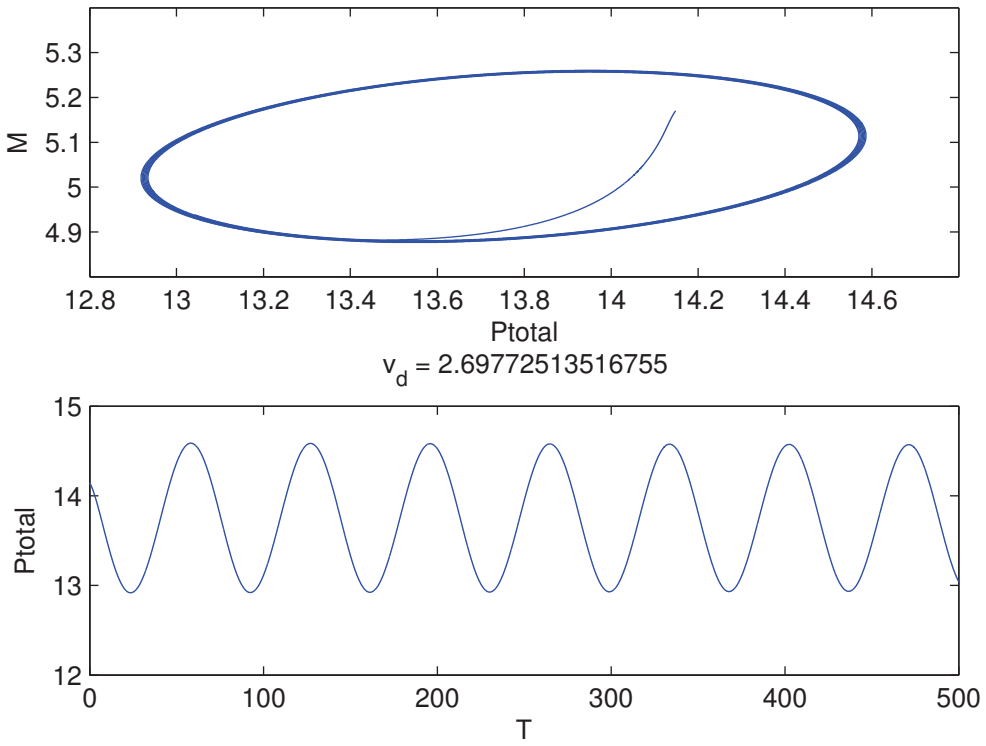

Before the critical value $v_d = 2.69772513516755 - 1/10$

$$
\begin{aligned}
Fixed - point &= 4.88739451093913 \\
&= 8.71114868065035 \\
&= 1.78571147919427 \\
&= 0.501599389576917 \\
&= 0.733106800150879 \\
Eigenvalues &= -4.64312611073311 \\
&= -1.01341045785567 \\
&= 0.00155432482574324 + 0.107127285380774i \\
&= 0.00155432482574324 - 0.107127285380774i \\
&= -0.386248006669926
\end{aligned}
$$

And corresponding plots are:

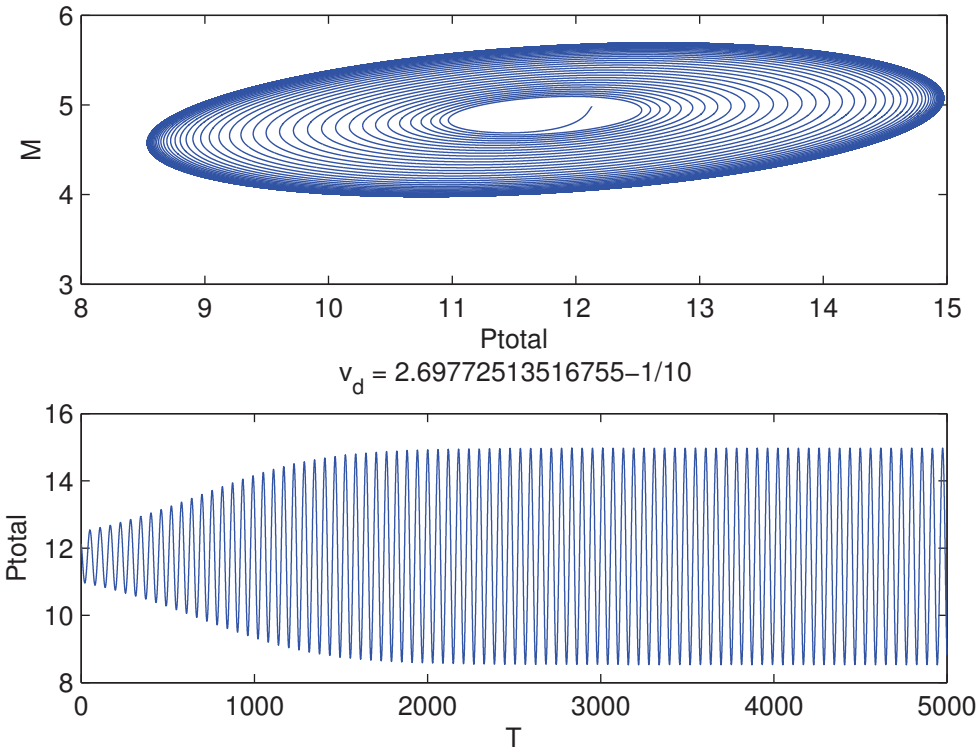

It is clear that the real parts of complex eigen-values are positive, so fixed point is repealer. Integrating the system in the neighborhood of fixed point shows convergent behaviour towards limit cycle.

After the critical value $v_d = 2.69772513516755 + 1/10$

$$
\begin{aligned}
Fixed - point &= 5.25269783077853 \\
&= 13.3938625154428 \\
&= 1.99103194495107 \\
&= 0.497948179269186 \\
&= 0.727770415854966 \\
Eigenvalues &= -4.70511092679921 \\
&= -0.947549456895608 \\
&= -0.00134745762309573 + 0.0751054115264168i \\
&= -0.00134745762309573 - 0.0751054115264168i \\
&= -0.357640766703895
\end{aligned}
$$

And corresponding plots are:

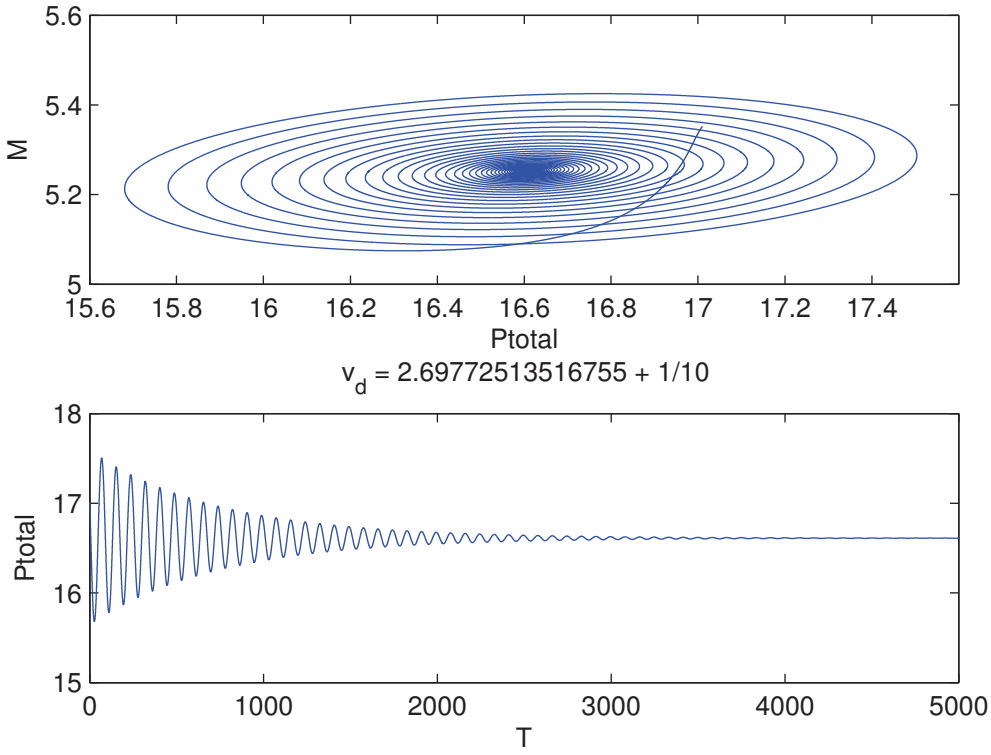

It shows that all the real parts of eigenvalues are negative, so the fixed point becomes attractor and this means that the limit cycle bifurcates.

4.5 A note on finding Hopf-bifurcation point

As shown in section 2, the Jacobi matrix has three negative and a pair of purely imaginary eigenvalues implies that $A_1 > 0, A_2 > 0$ and $A_3 = 0$. Hence the parameters such that $A_3 = 0$ are candidates for the Hopf bifurcation. The numerical simulations given above show that $v_s = 0.637930420865621$ results in a pair of complex conjugate eigenvalues which are very close to the imaginary axis. Thus this can be considered as a Hopf bifurcation point. However numerical computations show that $A_1 > 0$, $A_2 > 0$ and $A_3 = 0.0000551355$. It can be seen that A_3 is close to but not very close to zero.

4.6 D-curve

Consider the equation

$$f_0(x) + f_1(x)u_1 + f_2(x)u_2 = 0 \tag{47}$$

Assume $f_0, f_1, f_2 \in C^2$ and $f_1^2(x) + f_2^2(x) \neq 0$ for all $x \in \mathbb{R}$. To determine the number and values of solutions of this equation at a given parameter pairs (u_1, u_2) consider the set

$$S = \{(u_1, u_2) \in \mathbb{R}^2 : \exists x \in \mathbb{R} \text{ such that } f(x, u_1, u_2) = f'(x, u_1, u_2) = 0\}.$$

Let $W = \{x \in \mathbb{R} : f_1(x)f_2'(x) - f_1'(x)f_2(x) \neq 0\}$. The curve $D : W \to \mathbb{R}^2$ defined by

$$D_1 = \frac{f_2(x)f_0'(x) - f_2'(x)f_0(x)}{f_1(x)f_2'(x) - f_1'(x)f_2(x)} =: u_1 \quad D_2 = \frac{f_0(x)f_1'(x) - f_0'(x)f_1(x)}{f_1(x)f_2'(x) - f_1'(x)f_2(x)} =: u_2$$

is called D-curve (or discriminent curve) belonging to the bifurcation problem (47). A simple calculation gives us the coordinates of the tangent vector $D'(x)$

$$\begin{aligned} D_1'(x) =& f_2(x)\frac{f_0''(x) + f_1''(x)D_1(x) + f_2''(x)D_2(x)}{f_1(x)f_2'(x) - f_1'(x)f_2(x)}, \\ D_2'(x) =& -f_1(x)\frac{f_0''(x) + f_1''(x)D_1(x) + f_2''(x)D_2(x)}{f_1(x)f_2'(x) - f_1'(x)f_2(x)} \end{aligned} \tag{48}$$

The following results can be found in [11].

Proposition 4.5. *Assume that*

(H1) $f_0, f_1, f_2 \in C^2$ *and* $f_1^2(x) + f_2^2(x) \neq 0$ *for all* $x \in \mathbb{R}$,

(H2) $\mathbb{R} \setminus W$ *consists isolated points;*

(H3) $\{x \in \mathbb{R} : f_0''(x) + f_1''(x)D_1(x) + f_2''(x)D_2(x) = 0\}$ *consists of isolated points.*

Then

(a) the tangent unit vector of the D-curve $e(x) = D'(x)/\|D'(x)\|$ is defined on $\mathbb{R}$ except at isolated points;

(b) For every $x_0 \in \mathbb{R}$ there exists the left and right limits.

Definition Let $x_0 \in \mathbb{R}$ be a point and let ℓ be a line on the parameter plane with $A_0 + A_1u_1 + A_2u_2 = 0$. This line is called a tangent line of the D-curve at x_0 if $\lim_{x\to x_0} \operatorname{dist}(D(x), \ell) = 0$ (dist. stands for the distance), and the left and right limits are orthogonal to (A_1, A_2), the normal vector of ℓ.

Note that x_0 is not assumed to belong to W. Thus the definition is an extention of the usual tangent. In the case $x_0 \in W$ they are identical. Let

$$M(x) = \{(u_1, u_2) \in \mathbb{R}^2 : f(x, u_1, u_2) =\}.$$

Theorem 4.6 (Tangential property)**.** *Under conditions (H1)-(H3) for any $x_0 \in \mathbb{R}$ the line $M(x_0)$ is a tangent of the D-curve at x_0.*

Theorem 4.7 (Convexity property)**.** *Assume that conditions (H1)-(H3) hold. Let $x_0 \in W$. If $f_0''(x) + f_1''(x)D_1(x) + f_2''(x)D_2(x)$ changes its sign at x_0, then the D-curve has a cusp point at x_0, i.e. $\lim_{x\to x_0^-} e(x) = -\lim_{x\to x_0^+} e(x)$. If $f_0''(x) + f_1''(x)D_1(x) + f_2''(x)D_2(x)$ does not change its sign at x_0, then the D-curve is locally on the left (right) side of its tangent belonging to x_0 if $f_1(x)f_2'(x) - f_1'(x)f_2(x)$ is positive (negative).*

As computed earlier (see Section 2)

$$ax^{n+1} + bx + c = 0.$$

Now $f_0(x) = ax^{n+1}$, $f_1(x) = 1$, $f_2(x) = x$ and b and c are bifurcation parameters. So the functions f_0, f_1, f_2 are C^2-functions and satisfy $f_1^2(x)+f_2^2(x) = 1+x^2 \neq 0$ thus (H1) holds. $f_1(x)f_2'(x) - f_1'(x)f_2(x) = 1$ and f_1, f_2 have finite number of zeros.

$$f_0''(x) + f_1''(x)D_1(x) + f_2''(x)D_2(x) = f_0''(x) = an(n+1)x^{n-1}$$

whose roots are isolated. The D-curve is

$$c = D_1(x) = anx^{n+1}, \quad b = D_2 = -(n+1)ax^n.$$

Its derivative is

$$D'(x) = f_0''(x)(x, -1) = a(n+1)nx^{n-1}(x, -1),$$

Therefore the tangent line of the D-curve at the point $D(x)$ is the line with direction vector $(x, -1)$. This line is called $T(x)$. The tangential property yields that a number x is a solution of $ax^{n+1}+bx+c = 0$ for any point (c, b) if and only if $(c, b) \in T(x)$. In other words $T(x) = M(x)$. Thus for any point (c, b) in the parameter plane, the number of the solutions of the equation under consideration equals to the number of the tangent lines that can be drawn from (c, b) to the D-curve. Moreover, the value of the solutions can be considered as the value of x at the tangent point. According to the convexity property the D-curve contains convex arcs. Now $\mathbb{R} = W$. These arcs can join together only in cusp points. The cusp point is $x = 0$ computed from from $f_0''(x) = 0$. Furthermore, the convexity

of the separate arcs means that they completely lie on one side of the tangent line belonging to any point of the arc.

In this particular case, the following conclusion can be drawn.

Theorem 4.8. *(a) The D-curve has a cusp point at the parameter value x if and only if n is even.*

(b) If n is odd then the D-curve is locally on the left side of its tangent at x (the left normal vector of the curve is obtained by a counterclockwise rotation from $D'(x)$).

(c) For n even $f_0''(x)$ does not change sign in the interval $[0,\infty)$ and n odd $f_0''(x)$ does not change sign for all $x \in \mathbb{R}$. Thus for any parameter pair (c,b) the number of tangents which can be drawn from (c,b) to the arc of the D-curve belonging to the interval $[0,\infty)$ for even n and $\mathbb{R}$ for odd n respectively is at most two.

For global bifurcation diagram it is computed that

$$\lim_{x\to-\infty} \frac{f_0(x)}{\sqrt{f_1^2(x)+f_2^2(x)}} = \begin{cases} -\infty & \text{if } n \text{ is even} \\ \infty & \text{if } n \text{ is odd} \end{cases}; \quad \lim_{x\to\infty} \frac{f_0(x)}{\sqrt{f_1^2(x)+f_2^2(x)}} = \infty$$

Then the global bifurcation diagram is a subset of the singular set S, i.e. the D-curve divides the parameter plane according to the number of solutions of $ax^{n+1}+bx+c=0$.

4.7 H-curve

The Jacobian matrix of the system is shown in Section 2. If this matrix has three negative real and a pair of purely imaginary eigenvalues then $A_3 = 0$, by Proposition 2.13. Then the Hopf-bifurcation takes place under this condition. Thus the H-curve in the (c,b)-plane is defined as

$$\begin{aligned} ax^{n+1}+bx+c &= 0 \\ A_3 &= 0 \end{aligned}$$

It is not possible to get an analytic expression for these parameters. One should be able to plot the H-curve by numerical calculation. However all the details are not worked here and this is left for further investigation.

5 Further discussions

Our original plan of this thesis was to give a bifurcation analysis of the five dimensional circadian model as complete as possible. During the working procedure we found that there were many unclear statements in the literature on systems biology. This made us to change the focus of our study. Our aim is to clarify some theories used in the analysis of biological models and we have tried

to verify the numerical results given in many papers by the theoretical analysis. Some of these are classical and some are not. Thus we have tried to study different theories on stability and bifurcation analysis and we exemplified by models of circadian rhythms which are popular subjects in recent research literature.

Our mathematical analysis based on numerical computations showed that several statements on Hopf-bifurcation are not completely correct. In turn we found that the numerically observed limit cycles are limit cycle bifurcated in the sense of Hopf.

Due to the time limit we are not able to work out details in Bautin bifurcation. In the case of Hopf bifurcation we have obtained a clear picture of bifurcation diagram. We have got better approximation for the Hopf bifurcation for five dimensional system.

We would like to point out that there seems to exist a powerful method in doing stability and bifurcation analysis using mathematical control theoretical approach. Such work is represented by Angeli and Sontag, and their co-workers (see e.g. [1]). The key concepts are monotone systems appearing naturally in models from systems biology and small gain theorem from robust analysis in control theory. One advantage of the small gain theorem is its robuestness with respect to all perturbations that preserve monotonicity and stability properties of a very low-dimensional model reduction. This robustness makes the technique useful in the analysis of molecular biological models in which there is large uncertainty regarding the values of kinetic and other parameters.

References

[1] D. Angeli and E. Sontag,*Oscillations in I/O monotone systems under negative feedback*, IEEE Transactions on Circuits and Systems, Special Issue on Systems Biology, **55** (2008)pp.166-176.

[2] L. Edelstein-Keshet, Mathematical Models in Biology, SAIM Classics in Applied Mathematics, 2005.

[3] Yuri A. Kuznetsov, *Elements Of Applied Bifurcation Theory*

[4] J. Guckenheimer and P. Holmes Nonlinear oscillations, dynamical systems, and bifurcations of vector fields, Springer Verlag, 1986.

[5] A. Goldbeter, *A model for circadian oscillations in the Drosophia period protein (PER)*, Proc. Royal Soc. London B., **261** (1995) pp.319-324.

[6] A. Goldbeter, Models for oscillations and excitability in biochemical systems. In *Mathematical Models in Molecular and Cellular Biology.* L.A. Segel, ed. Cambridge Univ. Press, Cambridge, pp. 248-291, 1980.

[7] H.K.Khalil, Nonlinear Systems. Prentice Hall, 3rd ed. 2002.

[8] J.-C. Leloup and A. Goldbeter. *A model for circadian rhythms in Drosophila incorporating the formation of a complex between PER and TIM proteins* J. Biol. Rhythms, **13** (1998) pp. 70-87.

[9] A. Goldbeter. *Computational approaches to cellular rhythms* J. Unite de Chronobiologie theorique, Faculte des Sciences, Universite Libre de Bruxelles, Campus Plaine, CP 231, B-1050 Brussels, Belgium

[10] B. Nagy, *Comparison of the bifurcation curves of a two-variable and a three variable circadian rhythm model*, Applied Mathematical Modelling, **32** (2008), pp.1587–1598.

[11] P.L. Simon, H. Farkas and M. Wittmann, *Constructing global bifurcation diagrams by the parametric representation method*, J. Computational and Applied Mathematics **108** (1999), pp.157-176.

[12] leecher777, *Drosophila Melanogaster Lab Report*

[13] J.J. Tyson, C.I. Hong, C.D. Thron and B. Novak, *A Simple Model of Circadian Rhythms Based on Dimerization and Proteolysis of PER and TIM*, Biophysical Journal, **77** (1999), pp. 2411-2417.

[14] Gantmacher, F.R., *Matrix Theory* Vol. II Chelsea Pub. Co. New york, 1964.

[15] Linda J.S. Allen, *Introduction to Mathematical Biology, An Pearson Education*
ISBN: 9780130352163

[16] Albert Goldbeter, Foreword by M. J. Berridge, *Biochemical Oscillations and Cellular Rhythms, The Molecular Bases of Periodic and Chaotic Behaviour*
online ISBN: 9780511608193

[17] Daniel B. Forger, Richard E. Kronauer, *Roconciling Mathematical models of biological clocks averaging on approximation manifolds*